The Journal of Neuroscience, April 1, 1999, *19*(7):2807–2822

A Neurocomputational Theory of the Dopaminergic Modulation of Working Memory Functions

Daniel Durstewitz, Marian Kelc, and Onur Güntürkün

Arbeitseinheit Biopsychologie, Ruhr-Universität Bochum, D-44780 Bochum, Germany

The dopaminergic modulation of neural activity in the prefrontal cortex (PFC) is essential for working memory. Delay-activity in the PFC in working memory tasks persists even if interfering stimuli intervene between the presentation of the sample and the target stimulus. Here, the hypothesis is put forward that the functional role of dopamine in working memory processing is to stabilize active neural representations in the PFC network and thereby to protect goal-related delay-activity against interfering stimuli. To test this hypothesis, we examined the reported dopamine-induced changes in several biophysical properties of PFC neurons to determine whether they could fulfill this function. An attractor network model consisting of model neurons was devised in which the empirically observed effects of dopamine on synaptic and voltage-gated membrane conductances could be represented in a biophysically realistic manner. In the model, the dopamine-induced enhancement of the persistent Na^+ and reduction of the slowly inactivating K^+ current increased firing of the delay-active neurons, thereby increasing inhibitory feedback and thus reducing activity of the "background" neurons. Furthermore, the dopamine-induced reduction of EPSP sizes and a dendritic Ca^{2+} current diminished the impact of intervening stimuli on current network activity. In this manner, dopaminergic effects indeed acted to stabilize current delay-activity. Working memory deficits observed after supranormal D1-receptor stimulation could also be explained within this framework. Thus, the model offers a mechanistic explanation for the behavioral deficits observed after blockade or after supranormal stimulation of dopamine receptors in the PFC and, in addition, makes some specific empirical predictions.

Key words: dopamine; prefrontal cortex; working memory; D1 receptor; theory; neurocomputation; delayed matching-to-sample

The prefrontal cortex (PFC) plays a major role in working memory (Passingham, 1975; Fuster, 1989; Goldman-Rakic, 1990, 1995; Petrides, 1995; Kesner et al., 1996). In a series of recent experiments, Miller and colleagues (Miller et al., 1991, 1993, 1996; Miller and Desimone, 1994) extended the classical delayed matching-to-sample (DMS) paradigm, which is often used to assess working memory functions, by introducing intervening stimuli between the presentation of the sample stimulus and the matching stimulus, after which a response had to be given. While monkeys were performing this task, these authors recorded from PFC neurons. As shown previously (for review, see Fuster, 1989; Goldman-Rakic, 1990), Miller et al. (1996) found that many neurons exhibited stimulus-selective delay-activity. In addition, in contrast to delay-active neurons in the temporal (Miller et al., 1993, 1996; Miller and Desimone, 1994) and posterior parietal (Di Pellegrino and Wise, 1993; Constantinidis and Steinmetz, 1996) lobe, delay-activity of most PFC neurons persisted even when intervening stimuli were presented. Thus, PFC neurons or networks seem to be equipped with a mechanism that enables them to hold active neural representations of goal-related information and to protect this goal-related delay activity against interfering stimuli. However, the nature of this neural mechanism is largely unknown.

We speculated that dopamine (DA) might play a crucial role in such a mechanism. Dopaminergic midbrain neurons become active (Schultz et al., 1993) and DA levels in the PFC significantly increase (Watanabe et al., 1997) during working memory performance. Prefrontal DA depletion (Brozoski et al., 1979; Simon et al., 1980) or blockade of D1 receptors in the PFC (Sawaguchi and Goldman-Rakic, 1991, 1994; Seamans et al., 1998) causes severe working memory deficits, whereas D1 agonists might enhance delay task performance [Arnsten et al. (1994); Müller et al. (1998); but see Zahrt et al. (1997)]. Moreover, DA strongly modulates the electrical activity of PFC neurons *in vivo* and *in vitro* by multiple D1- and D2-receptor-mediated presynaptic and postsynaptic mechanisms (Bernardi et al., 1982; Ferron et al., 1984; Mantz et al., 1988; Sesack and Bunney, 1989; Sawaguchi et al., 1990a,b; Godbout et al., 1991; Williams and Goldman-Rakic, 1995; Yang and Seamans, 1996). DA enhances a persistent Na^+ and reduces a slowly inactivating K^+ and a dendritic HVA Ca^{2+} current in rat PFC pyramidal neurons via D1 stimulation *in vitro* (Yang and Seamans, 1996; Gorelova and Yang, 1997; Shi et al., 1997), it reduces glutamatergic synaptic inputs (Pralong and Jones, 1993; Law-Tho et al., 1994), and it enhances activity and spontaneous transmitter release of GABAergic neurons in the PFC (Penit-Soria et al., 1987; Rétaux et al., 1991; Pirot et al., 1992; Yang et al., 1997). We asked whether DA by modulating these biophysical properties of PFC neurons could act to stabilize and protect goal-related delay-activity in PFC networks. To answer this question, we constructed a network of leaky-integrator model neurons that allowed for a biophysically realistic imple-

Received Oct. 15, 1998; revised Jan. 15, 1999; accepted Jan. 21, 1999.

This research was supported by grants of the Alfried Krupp-Stiftung (D.D., O.G.) and the Deutsche Forschungsgemeinschaft through its Sonderforschungsbereich NEUROVISION (O.G.). We are very thankful to Dr. Jean-Marc Fellous and to Dr. Jeremy Seamans for their helpful comments on this manuscript.

Correspondence should be addressed to Dr. Daniel Durstewitz, Salk Institute for Biological Studies, Computational Neurobiology Laboratory, 10010 North Torrey Pines Road, La Jolla, CA 92037.

mentation of the cellular effects of DA. Network simulations were performed, and the stability of representations was evaluated while DA-dependent neural and synaptic parameters were varied.

MATERIALS AND METHODS

Single neuron model. The goal of the present model was to explain the stability of delay-activity in the PFC and the dopaminergic modulation of this activity. We tried to keep the model as simple as possible within the constraints imposed by this goal. For example, because only average spike rates but not single spike codes are considered in the literature dealing with delay-activity during working memory and the dopaminergic modulation of this activity, spike rates were directly derived from membrane potential fluctuations in the model neurons instead of implementing an explicit spike-generating mechanism. On the other hand, we attempted to put sufficient detail into the equations to realistically describe the impact of DA on the state and behavior of the model neurons. For the purposes of the present study, we extended a network model extensively studied by Amit and colleagues (Amit et al., 1994; Amit and Brunel, 1995), who also showed that this model could reproduce very well various aspects of the electrophysiological behavior of neocortical neurons recorded *in vivo*.

The excitatory model neurons used in the present network study were intended to represent deep-layer PFC pyramidal cells. Layer V/VI pyramidal cells are the ones most densely innervated by dopaminergic fibers in the rat PFC (Berger et al., 1988, 1991; Joyce et al., 1993) and constitute the major portion of neurons with sustained delay activity (Fuster, 1973). To account for the electrotonically separated proximal (soma, basal, apical oblique) and distal (apical tuft) dendrites of these neurons, the model neurons were chosen to consist of a distal and a proximal "dendritic" compartment, connected by a coupling resistance, as depicted in Figure 1.

The proximal and distal compartments were described by simple "leaky-integrator" differential equations. The equation describing the proximal compartment contained additional nonlinear terms that represented the contribution of a persistent Na^+ (V_{NaP}) and a slowly inactivating K^+ (V_{KS}) current to the membrane potential:

$$\tau_p \dot{V}_{p,i} = -V_{p,i} + \eta_{exc} \sum_{j \neq i}^{N} w_{ij} f_{exc}(V_{p,j}) - \eta_{inh} f_{inh}(V_{inh}) + \lambda_{pd}(V_{d,i} - V_{p,i}) + V_{NaP}(V_{p,i}) + V_{KS}(V_{p,i}) \quad (1a)$$

$$\tau_d \dot{V}_{d,i} = -V_{d,i} + \eta_{exc} I_{aff,i} + \lambda_{pd}(V_{p,i} - V_{d,i}), \quad (1b)$$

where $V_{p,i}$ is the proximal and $V_{d,i}$ the distal membrane potential of unit i, τ_p the proximal and τ_d the distal membrane time constant, λ_{pd} a coupling strength between the proximal and the distal compartment (which may be interpreted as a length constant of the model neuron), η_{exc} and η_{inh} the general excitatory and inhibitory synaptic efficiency, w_{ij} the specific excitatory synaptic coupling strength (weight) from neuron j to neuron i, f_{exc} and f_{inh} the (instantaneous) firing rates of the excitatory neurons and the inhibitory unit, respectively, and I_{aff} represents an afferent input arising from other association or higher sensory areas (see below) (all variables in arbitrary units).

Because two of the major cellular effects of DA (see Implementation of the dopaminergic modulation) are on the persistent Na^+ (I_{NaP}) (Alzheimer et al., 1993; Brown et al., 1994; Yang and Seamans, 1996) and slowly inactivating K^+ current (I_{KS}) (Huguenard and Prince, 1991; Spain et al., 1991; Yang and Seamans, 1996), a simplified biophysical description of these currents was implemented in the model. Both currents activate on depolarization and were represented by the product of a maximum current ($I_{NaP,max}$ and $I_{KS,max}$, respectively) with a voltage-dependent (steady-state) activation gate, given by a sigmoid (Boltzmann) function (the slow inactivation process of these currents was omitted for simplicity). The change in membrane voltage induced by these currents relates to these currents by the constant passive membrane resistance R, which was set to 1.0 for simplicity (but could be set to any other value provided that the maximum currents are scaled accordingly):

$$V_{NaP}(V_p) = R\, I_{NaP}(V_p) = R\, I_{NaP,max}[1 + \exp(\beta_{NaP}(\alpha_{NaP} - V_p))]^{-1}$$
$$V_{KS}(V_p) = -R\, I_{KS}(V_p) = -R\, I_{KS,max}[1 + \exp(\beta_{KS}(\alpha_{KS} - V_p))]^{-1}. \quad (2)$$

Table 1. Model parameter settings

	χ	χ_{base}	χ_{shift}
Excitatory neurons	τ_{prox}	15.0	
	τ_{dis}	5.0	
	θ_{exc}	0.02	
	η_{exc}	0.25	−0.05
	λ_{pd}	0.7	−0.3
Na^+ current	$I_{NaP,max}$	0.09	
	α_{NaP}	0.06	−0.015
	β_{NaP}	50.0	
K^+ current	$I_{KS,max}$	0.045	−0.035
	α_{KS}	0.028	
	β_{KS}	30.0	
Inhibitory unit	τ_{inh}	1.0	
	θ_{inh}	0.055	
	η_{inh}	1.15	0.1
DA unit	τ_{DA}	150.0	
	θ_{DA}	0.015	
	γ_{DA}	1.0	
Motor unit	τ_{mot}	6.0	
	θ_{mot}	0.115	
	η_{mot}	−5.0	

For explanation of symbols, see Materials and Methods.

In the present paper, we were not seeking precise quantitative matches with empirical data. Rather our goal was to demonstrate some important functional principles that work regardless of the detailed activation kinetics (which are fast compared with the membrane time constants) or the exact parameter settings of the gating functions. For the present line of argument, the key point is that there are inward and outward currents in the model neurons that increase with membrane potential and could be differentially modulated by DA.

The spike frequency output f_{exc} of an excitatory neuron was set to zero below a certain threshold θ_{exc} and depended logarithmically on membrane potential above this threshold (as described by Amit and Brunel, 1995):

$$f_{exc}(V_p) = \begin{cases} \ln(V_p/\theta_{exc}) & \text{if } V_p > \theta_{exc} \\ 0 & \text{else} \end{cases}. \quad (3)$$

The population of GABAergic interneurons was lumped into a single inhibitory unit (Amit et al., 1994; Amit and Brunel, 1995). For this unit, membrane potential and spike frequency output were given by the following equations:

$$\tau_{inh} \dot{V}_{inh} = -V_{inh} + \frac{1}{N_S} \sum_{j}^{N} \eta_{exc} f_{exc}(V_{p,j}) \quad (4)$$

$$f_{inh}(V_{inh}) = \begin{cases} V_{inh} - \theta_{inh} & \text{if } V_{inh} > \theta_{inh} \\ 0 & \text{else} \end{cases},$$

where V_{inh} is the membrane potential, τ_{inh} the time constant, θ_{inh} the firing threshold of the inhibitory unit, and N_S the (mean) number of units coding for a stimulus (see below), introduced into the equation as a scaling constant.

A parameter configuration defining a "standard model" at baseline DA activity is summarized in Table 1 (column χ_{base}). Parameters regulating the maximum persistent Na^+ and slowly inactivating K^+ current, the maximum synaptic current, and the current flow between the two compartments were derived from simulations carried out with a detailed compartmental model of PFC pyramidal neurons (Durstewitz and Seamans, 1997; Durstewitz, 1998). We determined from this pyramidal cell model, which could faithfully reproduce somatic and dendritic recordings from real rat PFC neurons, the size of the total (subthreshold) I_{NaP}, the (subthreshold) axial current from the dendrites to the soma, and the

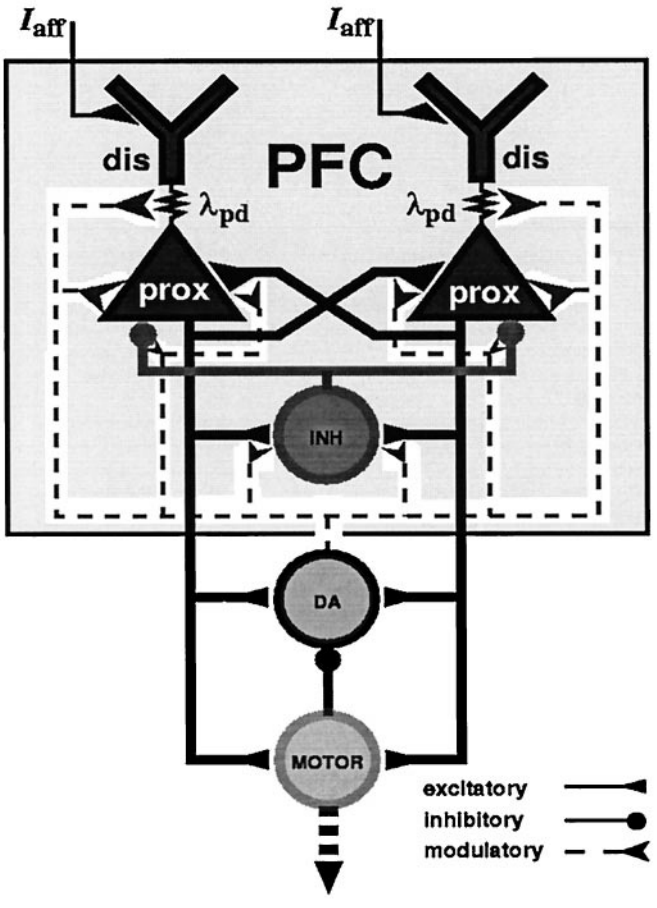

Figure 1. Structure of the PFC network model. Within the PFC network, excitatory neurons (representing deep-layer pyramidal cells) are interconnected by excitatory synapses on their proximal compartments (*prox*) while receiving afferent input from other cortices on their distal compartments (*dis*). An inhibitory unit (*INH*) provides feedback inhibition. A "striatal" motor unit (*MOTOR*) receives excitatory input from all PFC "pyramidal cells" and inhibits the "mesencephalic" DA unit, which modulates parameters of PFC neurons and synapses in an activity-dependent manner.

mean total synaptic currents (AMPA + NMDA, or $GABA_A$) under simulated "*in vivo*" conditions. We then used these values to adjust the relative contributions of these currents to membrane potential in the simple leaky-integrator neuron used here.

Network model. Figure 1 depicts the structure of the network model. The network consisted of a PFC layer, a motor output unit, and a DA unit. The PFC layer consisted of $N = 100$ excitatory "layer V/VI pyramidal neurons," arranged in a 10×10 square, and an inhibitory feedback unit, representing a population of GABAergic cells (Amit and Brunel, 1995). Within the PFC layer, each pyramidal cell made excitatory synaptic contacts only on the proximal compartments of other pyramidal neurons. In contrast, higher sensory afferent inputs (I_{aff} in Eq. 1b) were simulated by charging the distal model compartments. The inhibitory feedback unit received input from all pyramidal neurons and projected back onto the proximal compartments of all of those neurons. This pattern of connections was chosen according to neuroanatomical data. Lübke et al. (1996) and Markram et al. (1997) reported that deep-layer neocortical pyramidal cells made synaptic contacts on other deep-layer pyramidal cells preferentially within the proximal dendritic tree, and Kritzer and Goldman-Rakic (1995) and Levitt et al. (1993) showed that axonal arborizations of PFC deep-layer pyramidal neurons extending laterally across column boundaries mainly stayed within the same deep layers. In contrast, Mitchell and Cauller (1997) showed that afferent fibers from other cortical association and higher sensory areas terminate in the upper PFC layers I–II, which seems to be a common pattern of association fiber connections in the neocortex (Jones, 1984; Cauller, 1995; Cauller et al., 1998). Finally, axons from Chandelier and basket GABAergic interneurons primarily terminate on the initial axonal segment, soma, and proximal dendrites (i.e., the proximal compartment) of deep-layer pyramidal cells (Douglas and Martin, 1990). However, it should be emphasized that all of the results presented here except the ones regarding dopaminergic modulation of dendritic Ca^{2+} currents (see Results) do not depend on these anatomical assumptions.

In the Miller et al. (1996) task, which will be used here for the simulations, the monkeys gave their responses by pressing a lever. Thus, suprathreshold activity of the motor output unit in the present simulations was meant to indicate such a lever press. The motor output and the DA unit consisted of just one compartment as described by Equation 1a, without the terms for voltage-gated and axial current flow and without inhibitory feedback. Parameters for these units are given in Table 1. The motor unit received (nonreciprocal) connections from all PFC pyramidal neurons, with a fixed total weight $\eta_{exc} \times w = 1/(10 \times N_S) = 0.005$, where $N_S = 20$ is the number of neurons participating in the representation of a given stimulus (see below). This connection in the model network corresponds to the unidirectional glutamatergic fiber connections from PFC layer V pyramidal cells to striatal neurons (Selemon and Goldman-Rakic, 1985; Goldman-Rakic, 1995; Heimer et al., 1995).

The DA unit received excitatory input from all PFC pyramidal neurons, with a fixed total weight $\eta_{exc} \times w = 1/(10 \times N_S) = 0.005$, and inhibitory input from the motor unit with fixed weight $w = 1.0$ ($\eta_{mot} = -5.0$). Glutamatergic projections from the PFC to the substantia nigra (SN) have been demonstrated by glutamate uptake and ablation studies (Carter, 1982; Kornhuber et al., 1984). In addition, it has been shown that electrical and chemical stimulation of the PFC induces burst firing in the ventral tegmental area (VTA) and SN dopaminergic neurons (Murase et al., 1993; Tong et al., 1996a,b), which resembles natural burst events as elicited by behaviorally significant stimuli (Schultz and Romo, 1990; Ljungberg et al., 1992; Schultz et al., 1993). Burst firing in turn (as opposed to a single spike mode) leads to increased DA release at dopaminergic terminals in the forebrain (Gonon, 1988). Thus, PFC activity can stimulate DA release via direct or indirect (Tong et al., 1996a) excitatory fiber connections to the VTA/SN (Karreman and Moghaddam, 1996), justifying the assumptions made here.

The inhibitory signal from the motor unit to the DA unit represented the GABAergic input that SN and VTA dopaminergic neurons receive via the striatonigral pathway (Heimer et al., 1995). In an operant feeding task carried out by Nishino et al. (1991), VTA neurons increased their firing rate initially while monkeys pressed a lever for food reward but became inhibited thereafter during ingestion, i.e. when the goal has been achieved (see also Richardson and Gratton, 1998). Goldman-Rakic et al. (1992a) speculated that in an oculomotor delayed-response task, a command signal that originates in the PFC activates neurons in the striatum, which in turn inhibit the SN (Hikosaka and Wurtz, 1983), which finally results in disinhibition of the medial dorsal thalamic nucleus and superior colliculus. Thus, PFC neurons could directly excite dopaminergic midbrain neurons and stimulate DA release, or could inhibit them indirectly by initiating a motor output that results in goal achievement.

The kind of implementation outlined above was chosen to demonstrate the functioning of a completely self-regulating system. However, for the central ideas pursued in this paper, it does not matter whether the PFC itself activates the DA unit, whether it is activated by some other brain structure (e.g. the amygdala; Goldstein et al., 1996), or whether increased DA release in the PFC during working memory is regulated at the terminal level (Blaha et al., 1997), as long as it is provided that prefrontal DA levels rise at the onset of the working memory task [for a discussion of related points see Schultz (1992)]. Evidence for this comes (1) from the *in vivo* studies by Schultz et al. (1993), who demonstrated that VTA/SN neurons increase their firing rate with the presentation of the first, instructing stimulus in a spatial delayed response task, and (2) from Watanabe et al. (1997), who observed increased DA levels especially in the dorsolateral PFC of monkeys during performance of a delayed alternation but not during a sensory-guided control task.

Synaptic connections within the PFC layer and neural representation of stimuli. A number of different patterns, representing different environmental stimuli, were stored in the synaptic weight matrix of the network by connecting the neurons coding for a particular stimulus by high synaptic weights. For simplicity, patterns were represented by binary

vectors $\mathbf{S} = \{s_i\}$, and were stored in the PFC network according to a Willshaw matrix (Amit and Brunel, 1995):

$$w_{ij} = \begin{cases} w & \text{if there exists a pattern } \mathbf{S} \text{ such that } s_i\, s_j = 1 \\ 0 & \text{else.} \end{cases} \quad (5)$$

For all simulations, the weights were set to $w = 1/(N_S - 1)$. All stimuli were represented by binary patterns with fixed coding level $c = N_S/N = 0.2$, where $N = 100$ is the total number of excitatory neurons in the PFC layer, and $N_S = 20$ as defined above [if different patterns are to be represented by varying numbers N_S of units, N_S in the equations above should be set to the average number of units participating in a pattern (see Amit and Brunel, 1995)]. For the purpose of illustrating general network performance, patterns forming integer numbers ("0," "1," . . .) were used as easily recognizable stimuli. All input patterns that were used during a simulation run were stored a priori in the synaptic weight matrix [for mechanisms of online learning, see Amit and Brunel (1995)]. In the simulations demonstrating general network performance, there were always 10 patterns stored in the weight matrix. However, different numbers of patterns, different coding levels, or the assumption of small, non-zero, randomly initialized weights (<10% of w as defined above) between all network units all yield the same basic results (using parameters as given in Table 1). For different coding levels, only the weights have to be adjusted according to N_S as described above.

Stimuli (input patterns) were presented to the net by directly charging the distal compartments of the PFC layer pyramidal neurons (i.e., clamping I_{aff} in Eq. 1b). It is generally assumed that the increased firing rate of PFC neurons during the delay periods of working memory tasks represents the active holding of stimuli (Fuster, 1989; Goldman-Rakic, 1990, 1995; Funahashi and Kubota, 1994). Likewise, in the present network model, the active holding, or active short-term representation, of stimuli was reflected in the elevated firing rates of the neurons participating in the neural representation of the respective stimulus (Amit, 1995; Amit et al., 1997). Thus, different stimuli activated different representations encoded in the synaptic weight matrix of the network, which were then eventually maintained by recurrent excitation and thus transformed into active working memory representations. Amit and Brunel (1995) expressed conditions under which increased firing rates will be maintained in the absence of external input in associative networks of the type used here.

Implementation of the dopaminergic modulation. In the PFC, pyramidal cells seem to be the preferential targets of dopaminergic afferents and the major cell population expressing the D1-receptor-related phosphoprotein DARPP-32 (Goldman-Rakic et al., 1989; Berger et al., 1990; Smiley and Goldman-Rakic, 1993). However, dopaminergic inputs to smooth stellate and thus probably GABAergic interneurons and D1-like immunoreactivity in these neurons have also been observed (Smiley and Goldman-Rakic, 1993; Muly et al., 1998). In the rat PFC, layers V–VI receive the densest dopaminergic input, and in monkeys, in addition, the superficial (supragranular) cell layers (Berger et al., 1988, 1991; Goldman-Rakic et al., 1992b; Lewis et al., 1992). For simplicity we have assumed that biophysical parameters of *all* pyramidal neurons in these layers and thus in the model net are affected by DA [which seems also to be reasonably justified according to DARPP-32-positive cell countings in association areas of the avian "neocortex" (Durstewitz et al., 1998)].

DA has a variety of different effects on intrinsic membrane currents and synaptic parameters of pyramidal and GABAergic neurons in the PFC. We will focus here on the effects that are best documented. Furthermore, because the effects of DA on neural activity and single ion channels exhibit considerable substrate specificity [e.g., compare Cepeda et al. (1995) with Yang and Seamans (1996)], we will use in the present study only effects confirmed in rat PFC neurons. Dopaminergic actions considered in the present study were the following.

First, DA has been shown to enhance a persistent Na^+ current, probably by shifting the activation kinetics of this current into the hyperpolarized direction and by prolonging its inactivation time constant (Yang and Seamans, 1996; Gorelova and Yang, 1997). This effect might underlie the DA-induced depolarization of PFC neurons observed *in vitro* and *in vivo* (Bernardi et al., 1982; Yang and Seamans, 1996; Shi et al., 1997) and the dramatic increase in spike frequency (Yang and Seamans, 1996; Shi et al., 1997). In the model, this effect was implemented by shifting the activation curve of the persistent Na^+ current (i.e., parameter α_{NaP}) toward less positive potentials in a DA-dependent fashion (see below).

Recently, Gulledge and Jaffe (1998) reported that DA *reduces* the spike frequency of PFC pyramidal cells *in vitro*, in conflict with the findings cited above. The fact that Gulledge and Jaffe (1998) did not yet unravel the ionic mechanisms underlying this effect makes an assessment of its possible role in working memory processes very difficult. More importantly, these authors found that the depressive effect of DA is D2-mediated, whereas D1 receptor agonists and antagonists had no effect. In contrast, working memory performance (Arnsten et al., 1994; Sawaguchi and Goldman-Rakic, 1994; Zahrt et al., 1997; Müller et al., 1998; Seamans et al., 1998) and delay activity *in vivo* (Sawaguchi et al., 1990b; Williams and Goldman-Rakic, 1995) are mainly susceptible to D1 but not D2 receptor stimulation or blockade, as were the DA-dependent ionic mechanisms unraveled in the studies by Yang and Seamans (1996) and Gorelova and Yang (1997). In accordance with these findings, the D2-mediated depressive effect on spike frequency might only occur initially, shortly after bath application of DA *in vitro* (starting from a zero DA concentration), until the D1-mediated effects take over (J. Seamans, unpublished observations), and hence might not show up in an *in vivo* situation in which there is a constant baseline level of DA in the PFC (Abercrombie et al., 1989; Moore et al., 1998). Finally, D1 receptors are also much higher in density than D2 receptors in the PFC (Goldman-Rakic et al., 1992b; Joyce et al., 1993). Thus, the D2-mediated effects described by Gulledge and Jaffe (1998) might not play a prominent role in working memory processes, and we focused here on the D1-mediated effects elucidated by Yang and Seamans (1996) and Gorelova and Yang (1997).

Second, DA has been shown to reduce a slowly inactivating K^+ conductance (I_{KS}) in PFC pyramidal cells (Yang and Seamans, 1996). This effect might contribute to the depolarization and increased firing rate of PFC neurons under DA action. In the model, DA reduced $I_{KS,max}$ (see Eq. 2).

Third, DA reduces the amplitude and half-width of isolated dendritic Ca^{2+} spikes generated by a dendritic high voltage-activated (HVA) Ca^{2+} current (Yang and Seamans, 1996; Formenti et al., 1998). *In vitro* (Seamans et al., 1997) and compartmental modeling data (Bernander et al., 1994; Durstewitz and Seamans, 1997) have demonstrated that dendritic HVA Ca^{2+} currents can amplify EPSPs induced in the distal dendrites of deep layer PFC neurons on their way to the soma. In addition, Schiller et al. (1997) have shown that synaptic inputs to the distal dendrites activate local HVA Ca^{2+} currents, causing increased responses at the soma. Hence, dendritic HVA Ca^{2+} currents affect the ability of distal EPSPs to effectively depolarize the soma, and DA might reduce this ability. In addition, the data of Yang and Seamans (1996) made it likely that the DA-affected Ca^{2+} current resides primarily in the distal dendrites and might thus be of the N-type [more directly shown by Surmeier et al. (1995) and Formenti et al. (1998)], which reaches a local maximum in the distal dendrites of pyramidal cells (Westenbroek et al., 1992; Yuste et al., 1994). Thus, DA might specifically diminish distal EPSPs, or might at least attenuate them more strongly than proximal EPSPs [as first suggested by Yang and Seamans (1996)]. This has in fact been shown by Yang et al. (1996) and Law-Tho et al. (1994). The effect that DA induces via reduction of a dendritic Ca^{2+} conductance could be interpreted as an increase in the electrotonic distance between the distal and the proximal dendritic region, which causes a reduction in current flow from distal to proximal. Thus, in the model neurons, DA increased the electrotonic distance between the distal and the proximal compartment by reducing the coupling strength (λ_{pd}). However, in addition to this simple way of representing in the model dopaminergic effects on dendritic Ca^{2+} conductances, we also examined whether a more explicit representation of the DA-induced reduction of a dendritic Ca^{2+} current (see Results) basically yields the same results.

Fourth, in the PFC, as in other cortical areas (Pralong and Jones, 1993), DA depresses the AMPA as well as the NMDA component of EPSPs via D1 receptors (Law-Tho et al., 1994), thus reducing the amplitude of EPSPs evoked by layer I stimulation by up to 50%. Cepeda et al. (1992) also found that DA strongly suppresses glutamate-induced responses but reported enhanced responses to NMDA. (They did not, however, record from PFC neurons, and their slices were obtained from human brains that might have undergone pathological changes, so that the applicability of their results to the healthy PFC might have to be interpreted with some caution.) The suppressing effect of DA on glutamate-induced responses and EPSPs was implemented in the model by reducing the general excitatory synaptic efficiency η_{exc}.

Fifth, DA has been reported to enhance spontaneous activity of GABAergic interneurons and to increase IPSP size (Penit-Soria et al., 1987; Rétaux et al., 1991; Pirot et al., 1992; Yang et al., 1997). This effect, in addition to the DA-induced reduction of EPSPs, might be responsible

for the inhibition of neural activity in the PFC observed *in vivo* in anesthetized rats after local DA application or VTA stimulation (Ferron et al., 1984; Godbout et al., 1991; Pirot et al., 1992, 1996) (note that these studies were performed in rats anesthetized by ketamine, i.e., with NMDA currents blocked and outside a behavioral context). However, it should be noted that a reduction of *evoked* GABAergic activity and a reduction of IPSP sizes by DA in the PFC have also been reported (Rétaux et al., 1991; Law-Tho et al., 1994). We will show here what the effect of varying the general inhibitory synaptic efficiency η_{inh} on network behavior might be.

All of the DA-modulated network parameters were chosen to depend linearly on the deviation of the DA unit output from some baseline firing frequency. That is, with the DA unit firing at baseline, all network parameters had the values given in Table 1, and these values were varied according to the deviation Δf_{DA} of the DA unit output from some arbitrary baseline:

$$\chi(\Delta f_{DA}) = \chi_{base} + \chi_{shift} \times \Delta f_{DA}, \quad (6)$$

where χ denotes some network parameter, and χ_{base} and χ_{shift} are given for each DA-modulated parameter in Table 1. The deviation of the DA unit output from the baseline depended sigmoidally on the membrane potential of the DA unit, with a constant offset:

$$\Delta f_{DA} = (\gamma_{DA} + 0.5) \times [1 + \exp(200 \times (0.015 - V_{DA}))]^{-1} - 0.5, \quad (7)$$

where V_{DA} is the membrane potential of the DA unit, and γ_{DA} is a parameter normally set to 1.0 except for "pathological" conditions of DA hypoactivity (−DA condition, see below) or DA hyperactivity (++DA condition, see below). During the simulation runs demonstrating general network performance, the DA-induced parameter changes were roughly adjusted according to estimations derived from *in vitro* data (Law-Tho et al., 1994; Yang and Seamans, 1996) and to values obtained with simulations with a detailed compartmental model of PFC pyramidal cells (Durstewitz, 1998).

Testing the stability of working memory representations. To demonstrate the general performance of the PFC model network, the DMS task with intervening stimuli as used by Miller et al. (1993, 1996) and Miller and Desimone et al. (1994) was used here. An arbitrary sample pattern was first presented to the network by clamping distal afferent inputs (I_{aff} in Eq. 1b), followed by an arbitrary sequence of partly overlapping "intervening stimuli" (e.g., 4, 0, 0, 2, 4). The network had to respond, i.e., to activate the motor output unit, when the initially presented sample pattern appeared the second time (target condition). A new trial could then be started. Note that also a delayed *non*-matching-to-sample (DNMS) task could easily be implemented in the network by assuming that the initial sample pattern activates a representation of the target pattern (TP), i.e., evokes a representation of the goal state [as suggested, e.g., by the electrophysiological data of Quintana et al. (1988)]. This essentially would internally transform the DNMS problem into a DMS problem. It is also important to note that in the Miller et al. (1993, 1996) task, stimuli were *not* trial unique, i.e., intervening stimuli appeared as sample/target stimuli on other trials and were all known in advance to the animals, raising the opportunity for considerable interference between trials and stimuli and justifying the a priori storage of stimuli in the present network.

The central hypothesis of the present paper was that DA stabilizes goal-related delay activity and protects it against interfering stimulation. To investigate the effect of the DA-induced parameter changes on stability of goal-related neural representations more systematically, the afferent input (I_{aff} in Eq. 1b) needed to disrupt the ongoing network activity (i.e., the current neural representation) was taken as an index for stability. The higher the afferent input needed to establish a new activity pattern (i.e., a new attractor state) in the PFC network, the more stable is the currently active neural representation. We termed this current $I_{aff,crit}$ in the following. In these simulations, a single (DA-dependent) network parameter was systematically varied while for each run a sample pattern was established in the isolated PFC network (no motor and DA unit), and the dependence of $I_{aff,crit}$ needed to override this pattern on the value of the respective parameter was determined. The afferent input was presented for a time long enough for the activity of the stimulated neurons to reach their approximate maximum.

Computational techniques. The simulation software was programmed in C++, and all simulations were run on a 200 MHz Pentium PC using LINUX, a UNIX version for PCs, as operating system. The whole system of differential equations was simultaneously solved by a fourth-order Runge-Kutta method or the semi-implicit extrapolation method as described in Press et al. (1992), yielding the same results for the error criterion used here.

RESULTS

General network performance

The central hypothesis put forward here was that the function of DA during working memory processing is to stabilize active neural representations, i.e., to maintain goal-related neural activity in the PFC even in the presence of interfering afferent stimulation. The simulations presented in Figure 2 demonstrate that (1) the DA-induced changes of biophysical parameters, taken all together, are appropriate for fulfilling this function, and (2) the prefrontal system via known anatomical connections could dynamically regulate its DA level to achieve the proposed function.

Figure 2*A* compares the activity of the pyramidal units of the PFC network under two different conditions of simulated dopaminergic activity during a simulated DMS task with intervening stimuli as outlined in Materials and Methods. In the first condition (+DA), the intact network as given by the configuration in Table 1 was used. In the second condition (−DA), the output of the DA unit (or, in other terms, the DA level in the PFC) was strongly diminished by reducing the scaling factor γ_{DA} in Equation 7 to 0.3. Another interpretation of this manipulation might be a partial blockade of DA receptors in the PFC.

Figure 2*A* shows the mean membrane potential of all model neurons participating in the representation of a pattern that was the target in the first trial (TP1), and of all neurons participating in the representation of a pattern that was the target in the second trial (TP2). The first target served as an intervening stimulus (IS) during the second trial (i.e., IS4 = IS5 = TP1), and the second target as an intervening stimulus during the first trial (i.e., IS1 = IS2 = TP2). All patterns were presented by injecting $I_{aff} = 0.55$. Membrane potential instead of mean frequency output f_{exc} was chosen for visualization to depict also the subthreshold activity of the units not participating in the representation of the actual TP, and to allow comparison of this activity with that of the TP units. Because spike frequency in the model units relates logarithmically (i.e., strictly monotonically) to membrane potential above threshold, essentially the same picture would have been obtained for mean frequency of the TP units. Furthermore, for discrete time points during the first trial when the TP or one of the intervening stimuli was presented, the gray level-coded activity of all 100 network units is depicted.

As can be seen from Figure 2*A*, in the +DA network, activity related to the TP stayed stable during the whole trial even at times where interfering stimuli were presented to the network. Note that the mean activity of the delay-active units temporally increases during presentation of each of the intervening stimuli and reaches a maximum with the second presentation of the TP. This same basic pattern has been observed *in vivo* for single PFC neurons as well as for the mean frequency of a sample of delay-active neurons (Miller et al., 1996, their Figs. 4, 5), indicating that the model net could reproduce very well the basic electrophysiological pattern of delay-active neurons in the monkey PFC during DMS tasks with intervening stimuli. The increased firing rate during the second presentation of the target, which was termed "match enhancement" by Miller et al. (1996) and was observed in the majority of monkey PFC neurons with significant delay activity, triggered a suprathreshold motor output (Fig. 2*B*). Thus, the motor unit received suprathreshold activation only when a goal-

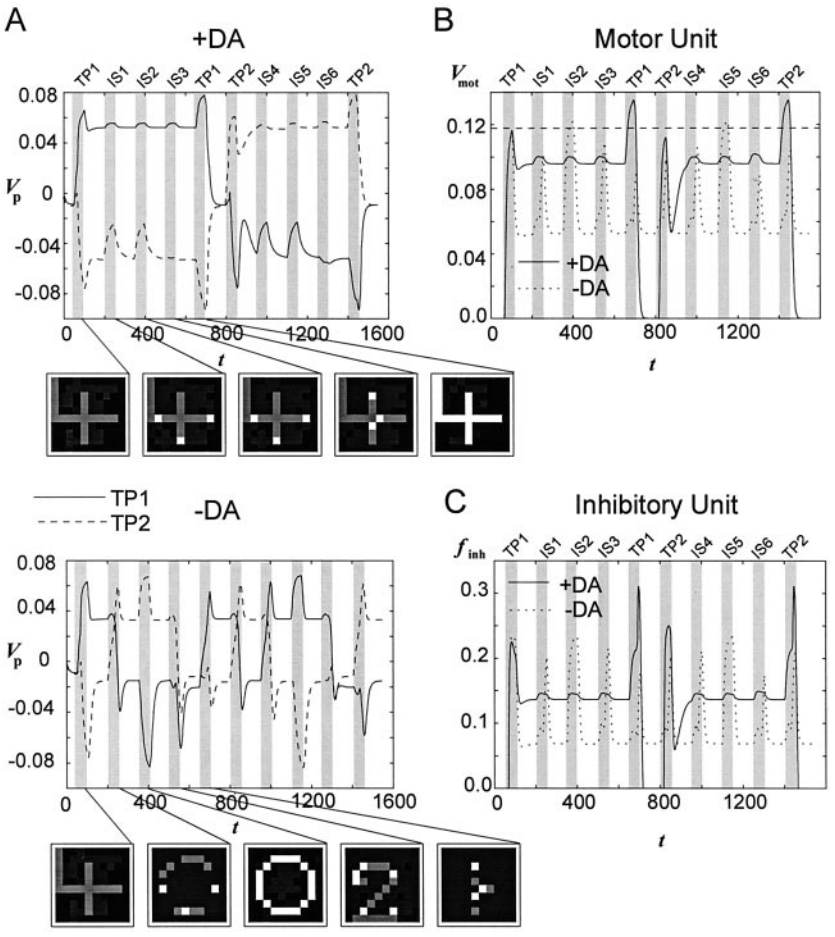

Figure 2. Activity of the PFC network under conditions of normal (*+DA*) and reduced (*−DA*) DA unit output during two successive trials of a DMS task with intervening stimuli. *A*, Mean proximal membrane potential (*top parts*) of all PFC net units belonging to the pattern "4," which is the TP in the first trial (*TP1*), and pattern "0," which is the TP in the second trial (*TP2*). *Gray bars* indicate the time intervals during which stimuli were presented. Three intervening stimuli (*IS1–IS3* and *IS4–IS6*, respectively) were presented between the first (sample) and the second (matching) presentation of a TP. Note that *IS1* = *IS2* = *TP2* and *IS4* = *IS5* = *TP1*. *Bottom parts* give the *gray* level-coded membrane potential of all 100 PFC network units at discrete time points during presentation of the stimuli in the first trial. *Lighter gray levels* indicate higher activity. With normal DA output, TPs stay stable during a whole trial (*+DA*), whereas intervening patterns override currently active patterns under conditions of reduced DA unit output (*−DA*). $I_{aff} = 0.55$. *B*, Membrane potential of the motor unit under the *+DA* and the *−DA* conditions. *C*, Mean firing frenquency of the inhibitory unit under the *+DA* and the *−DA* condition.

related match occurred. [In this sense the motor unit encoded a "pure match" as it has been observed for some neurons by Miller et al. (1996)]. As described by Miller et al. (1996), simple repetition of a stimulus (IS1 = IS2, IS4 = IS5 in Fig. 2*A*) or intervening presentation of a stimulus that was the target in other trials (IS1 = TP2, IS4 = TP1 in Fig. 2*A*) did not disrupt delay activity. However, after the motor response had been delivered, the strong inhibition of the DA unit enabled the transition to and active storage of a new TP.

For the −DA condition, the situation was quite different. The first intervening pattern wiped out the target-related delay activity, preventing any significant match enhancement effect and thus disabling correct motor output (Fig. 2*B*). Thus, in the model network the DA-induced parameter changes were a necessary prerequisite for the protection of goal-related delay activity against interfering afferent stimulation.

Figure 2*B* illustrates that a motor response during the DMS simulation depicted in Figure 2*A* is delivered only in the +DA model when a match between sample and target stimulus occurred. Figure 2*C* shows that the activity of the inhibitory unit closely mimics that of the excitatory model neurons. Furthermore, the activity of the inhibitory unit is higher in the +DA condition than in the −DA condition because of the increased firing frequency of the excitatory units.

Having demonstrated that DA, in principle, could subserve the proposed function, we will investigate in the next sections in detail which of the DA-modulated biophysical mechanisms could lead to stabilization of goal-related neural representations in working memory.

Contribution of the persistent Na^+ current to stabilization of delay activity

The DA-induced shift of the I_{NaP} activation curve (i.e., parameter α_{NaP}) toward less positive potentials makes the currently active representation more stable in terms of the afferent input needed to disrupt the current delay activity (see Materials and Methods) (Fig. 3). This generally holds for different steepnesses of the I_{NaP} activation function (data not shown), for different degrees of overlap between the target and the intervening pattern (Fig. 3*A*), and for different degrees of "connectivity" (Fig. 3*B*).

The term "overlap" (*OVL*) denotes the number of pyramidal units shared by the target stimulus and the intervening stimulus representation. As is evident from Figure 3*A*, increasing the overlap of the intervening stimulus with the TP reduces the afferent input needed to override the currently active pattern. However, no interaction of overlap with the I_{NaP} amplitude or activation threshold is apparent. Dashed vertical lines in Figure 3 illustrate in which range α_{NaP} varies within the full network simulation as depicted in Figure 2.

By connectivity (*CON*) we mean the number of inputs that units of the intervening pattern receive from the TP units, and vice versa. For the calculation of this index, all connections including units participating in the representation of *both* patterns (i.e., the overlapping units) were excluded. Thus, the connectivity as defined here depends solely on the other patterns stored in the network. In the extreme case, if there is a very large number of patterns stored in the network that overlap with the TP and the intervening pattern, each unit of the intervening pattern might

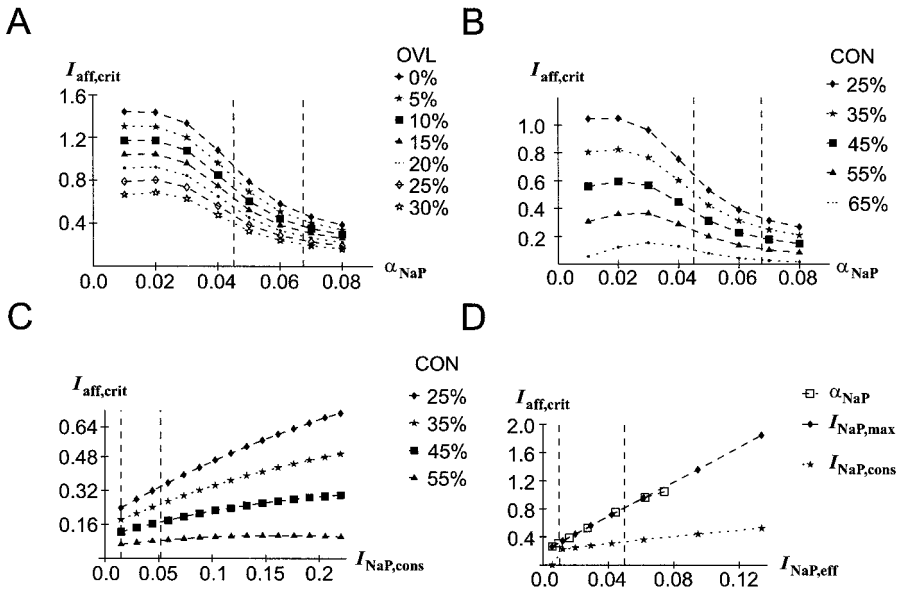

Figure 3. Effects of DA-induced variations in I_{NaP} parameters on the stability of TPs. Stability is measured in terms of the afferent input needed to disrupt current neural representations ($I_{aff,crit}$). *Dashed vertical lines* indicate the range within which the respective parameters or variables during full network simulations varied. All other network parameters had the baseline values given in Table 1. *OVL*, Overlap; *CON*, connectivity. *A*, Reduction of the I_{NaP} activation threshold (α_{NaP}) increases the stability of the active neural representation at different overlaps (*CON* = 25%). *B*, Reduction of the I_{NaP} activation threshold (α_{NaP}) increases the stability of the active neural representation at different connectivities (*OVL* = 15%). *C*, Dependence of the stability of an active representation on the amplitude of a constant (i.e., non-voltage-dependent) Na^+ current at different connectivities (*OVL* = 15%). *D*, Dependence of the stability of an active representation on the effective I_{NaP} amplitude ($I_{NaP,eff}$), compared for the constant I_{NaP} (labeled $I_{NaP,cons}$), for $I_{NaP,max}$ variation of the voltage-dependent I_{NaP} (labeled $I_{NaP,max}$), and for α_{NaP} variation of the voltage-dependent I_{NaP} (labeled α_{NaP}). *OVL* = 15%; *CON* = 25%.

receive inputs from *all* pattern units (and vice versa). Thus, the number of inputs may vary between 0 and N_S, and CON was expressed as percentage of the maximal number of possible inputs N_S. Furthermore, the connectivity between the target and the intervening pattern was always fully symmetrical. If the connectivity is too high, too many network units may become simultaneously active so that the TP breaks down because the stable membrane potential is temporarily pushed below the excitatory threshold by the increased inhibitory feedback (note from Equation 10 in the appendix that for $\eta_{inh} > 1$ the inhibitory feedback increases more steeply with rising mean frequency f_{exc} than the excitatory feedback). This in general was the case for CON $\geq$70% in the present network (depending on the specific settings of the parameters). Thus, only values of CON <70% were used in the present simulations. In general, also for CON <70%, increasing the connectivity diminishes stability (as evident in Fig. 3*B*) because the non-TP units receive more excitation whereas nothing changes for the TP units as long as $f_{exc} = 0$ for the non-TP units.

The DA-induced shift in the I_{NaP} activation function enhances I_{NaP} in the normal potential range of the excitatory neurons, and thus provides an additional source of current. Figure 3*C* demonstrates that this additional current alone, within a wide range of reasonable I_{NaP} amplitudes, could be sufficient for stabilizing current delay activity. That is, neglecting the voltage dependency of I_{NaP} and representing the dopaminergic modulation of I_{NaP} just by adding a *constant* $I_{NaP,cons}$ to *all* excitatory neurons suffices to make the representation more stable in the PFC network. This, again, holds for various degrees of overlap between the target and the intervening pattern (data not shown), and for various connectivities (Fig. 3*C*). As shown more analytically in the appendix, an additional excitatory current pushes the stable frequency of the delay-active neurons to higher values. Concurrently, the difference in membrane potential between the TP and the non-TP units increases (see Appendix). As indicated by simulation results (data not shown), within the range of $I_{NaP,cons}$ amplitudes examined here, the rise in the firing rate of the TP units via increasing the inhibitory feedback causes a decrease in the membrane potential of the non-TP units. Thus, higher afferent inputs are needed to drive these units above threshold; that is, it becomes more difficult for intervening stimuli to override the currently active neural representation. However, if $I_{NaP,cons}$ becomes too big, there is again a downward trend in stability (evident from Fig. 3*C* as a slight downward bend in the curve for the highest connectivity). This occurs when $I_{NaP,cons}$ becomes high enough to push also the non-TP units closer to threshold (despite the increased inhibition), especially in concert with high connectivities. Nevertheless, within a reasonable range of I_{NaP} amplitudes, the pure enhancement of I_{NaP} attributable to DA action could be a major determinant of the stabilizing effect.

The voltage dependency of I_{NaP} as implemented in the present model neurons makes an additional contribution to the stability of currently active representations. This is shown in Figure 3*D*, where the afferent input needed to disrupt the actual pattern is compared for the constant I_{NaP} and the voltage-dependent I_{NaP} as implemented here. To compare these two conditions, the respective $I_{NaP,cons}$ values were set to exactly the same values that the voltage-dependent I_{NaP} of the delay-active neurons had at the time when the afferent input was injected (termed $I_{NaP,eff}$ here), while $I_{NaP,max}$ was varied (for the constant I_{NaP}, $I_{NaP,eff} = I_{NaP,cons} = I_{NaP,max}$; for the voltage-dependent I_{NaP}, $I_{NaP,eff} \leq I_{NaP,max}$). Furthermore, shifting the I_{NaP} activation threshold α_{NaP} toward less positive potentials essentially has the same effect as increasing $I_{NaP,max}$, as illustrated in Figure 3*D*. Only for very high effective I_{NaP} amplitudes, shifting the threshold becomes less efficient than increasing $I_{NaP,max}$. Note also that for the threshold variation simulations, $I_{NaP,eff}$ is limited by $I_{NaP,max} = 0.09$.

The additional stabilizing effect of the voltage-dependent I_{NaP} compared with a constant current $I_{NaP,cons}$ is attributable to the fact that I_{NaP} increases with membrane potential and does so steeper for higher potentials (unless α_{Na} becomes very low). As a consequence, if α_{NaP} is reduced, there is a bigger increase in I_{NaP} in the TP units that reside at a higher membrane potential than in the non-TP units. Thus, reducing α_{NaP} not only increases an excitatory membrane current but in addition enlarges the difference in I_{NaP} activation between the TP and the non-TP units. In Figure 3*B*, the points where the trend in stability reverses with decreasing α_{NaP} values indicate the points of maximum difference in I_{NaP} activation between the TP and the non-TP units. Below these points, the non-TP units gain more additional current than

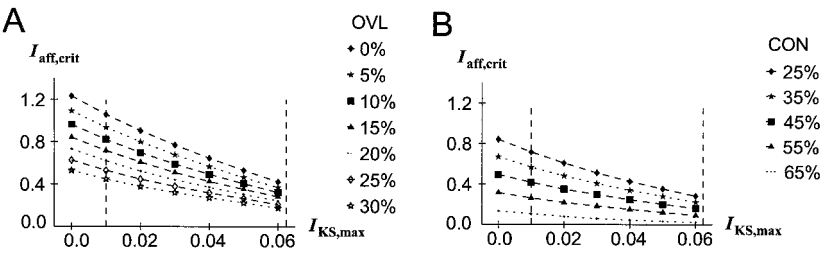

Figure 4. Effects of DA-induced variations in $I_{KS,max}$ on the stability of TPs (as measured by $I_{aff,crit}$). *Dashed vertical lines* indicate the parameter range within which $I_{KS,max}$ during full network simulations varied. All other network parameters had the baseline values given in Table 1. *OVL*, Overlap; *CON*, connectivity. *A*, Reduction of $I_{KS,max}$ leads to higher stability for different overlaps, more pronounced at low overlaps (*CON* = 25%). *B*, Reduction of $I_{KS,max}$ leads to higher stability for different connectivities, and this trend is more pronounced at low connectivities (*OVL* = 15%).

the TP units with decreasing α_{NaP} values. In general, whether a decrease in α_{NaP} results in an enlargement or a reduction of the difference in I_{NaP} activation between the TP and the non-TP units depends on whether the membrane potential of the TP or the non-TP units resides in a region of greater steepness of the sigmoid I_{NaP} activation function. In real neocortical pyramidal cells, this should always be the case for the membrane potential of the TP units because the point of maximum slope conductance (dI/dV) of the Na^+ currents lies well above firing threshold (Cummins et al., 1994; Fleidervish et al., 1996).

The persistent Na^+ current has been ascribed to a major role in synaptic amplification (Schwindt and Crill, 1995, 1996; Stuart and Sakmann, 1995). Basically, this view is fully compatible with the account given above. The model neurons are driven by excitatory synaptic inputs that activate I_{NaP} by pushing the membrane potential to higher levels. The amplification these synaptic inputs gain by activating I_{NaP} increases at higher membrane potential levels, so that the TP units profit more from a shift of α_{NaP}. However, one might argue that this is attributable to the fact that I_{NaP} was placed only into the proximal compartment (see Eq. 1), where the recurrent synapses terminate. Although this model assumption is completely justified by the results of Stuart and Sakmann (1995) and immunocytochemical data on the distribution of Na^+ channels by Westenbroek et al. (1989), it might not be well supported by the data of Schwindt and Crill (1995) and Mittmann et al. (1997), which suggest an amplification of distal EPSPs by I_{NaP} all along the apical dendrite. Hence, to rule out any possible objection one might base on a homogeneous dendritic distribution of I_{NaP}, the simulations shown in Figure 3*A,B* were rerun with model neurons where I_{NaP} was inserted also into the distal compartment (with the same properties as in the proximal compartment). The results were essentially the same, and the stabilizing effect was not less in magnitude than the one shown in Figure 3*A,B*.

Contribution of the slowly inactivating K^+ current to stabilization of delay activity

Because the slowly inactivating K^+ current like the persistent Na^+ current increases with membrane potential but acts in the opposite direction, reduction of its amplitude ($I_{KS,max}$) as induced by DA mirrors the effect that is produced by increasing the amplitude of I_{NaP}. TP representations become more stable at various overlaps with the intervening stimulus (Fig. 4*A*) and various degrees of connectivity (Fig. 4*B*) with decreasing values of $I_{KS,max}$. Just diminishing a source of (constant) negative current has a similar effect as an increase in $I_{NaP,cons}$. In addition, reducing $I_{KS,max}$ also results in a proportionally bigger decrease of the effective I_{KS} in the TP than in the non-TP units because of the fact that I_{KS} increases with depolarization (see Eq. 2). Another way to put this is that I_{KS} at higher membrane potentials more strongly withholds further depolarization induced by excitatory synaptic input, so that the TP units are affected to a bigger degree than the non-TP units by a partial removal of this current. As it was the case with the persistent Na^+ current, this stabilizing effect is generally robust with respect to other parameter settings, like that of the steepness of the I_{KS} activation function (β_{KS}), its threshold (α_{KS}), or the general excitatory synaptic efficiency (η_{exc}), although its magnitude depends on these parameters. We also verified that the stabilizing effect of $I_{KS,max}$ reduction still holds when I_{KS} is inserted into the distal dendritic compartment in addition to its proximal placement.

Contribution of the general excitatory synaptic efficiency to stabilization of delay activity

The effect of a reduction of the general excitatory synaptic efficiency (η_{exc}), which mimics the EPSP reduction observed after DA application *in vitro* (Pralong and Jones, 1993; Law-Tho et al., 1994), depends on the settings of the other network parameters and on the connectivity between the TP and the intervening stimulus. In particular, with the network model being in a low DA configuration (i.e., with all parameters assuming baseline values as given in Table 1), a reduction of η_{exc} only has a slightly stabilizing effect at different levels of overlap between the target and intervening pattern (Fig. 5*A*), and only at degrees (up to 50%) of connectivity that are not too high (data not shown). However, with all other parameters having values of a high DA configuration (i.e., assuming maximal DA unit output, $\Delta f_{DA} = 1.0$ in Equation 6), reduction of η_{exc} has a strongly stabilizing effect at different degrees of overlap (Fig. 5*B*). This effect is much more pronounced for low degrees of connectivity, and nearly absent at very high connectivities (Fig. 5*C*). Thus, reduction of the general excitatory synaptic efficiency has a consistently stabilizing effect only in concert with other DA-induced parameter changes. This is shown in more detail in Figure 5*D,E*, which demonstrates for a moderate degree of overlap (15%) and connectivity (25%) that the stabilizing effect of η_{exc} reduction increases with decreasing values of the I_{NaP} activation threshold (α_{NaP}) and decreasing values of the maximum I_{KS} amplitude ($I_{KS,max}$). Only for very low values of α_{NaP} does the effect reverse for the same reason mentioned in the section on I_{NaP}. At some point, decreasing α_{NaP} results in a decline of the difference in I_{NaP} activation between the TP and the non-TP units. The interaction of the DA-induced changes in η_{exc} with changes of I_{NaP} or I_{KS} is related to the fact that I_{NaP} amplifies and I_{KS} diminishes excitatory synaptic input. Mathematically, this relationship can be understood by explicating the stable frequency equation of the delay activity (see Appendix, Eq. 11), where η_{exc} enters in a divisive fashion into the V_{NaP} and V_{KS} terms.

Figure 5*F* demonstrates that in the high DA configuration the reduction of η_{exc} exerts its effect mainly but not exclusively by diminishing the impact of intervening stimuli on current network activity. Reducing the excitatory synaptic efficiency for the *internal* connections only while leaving it constant for the afferent input still leads to a small stabilizing effect for higher degrees of

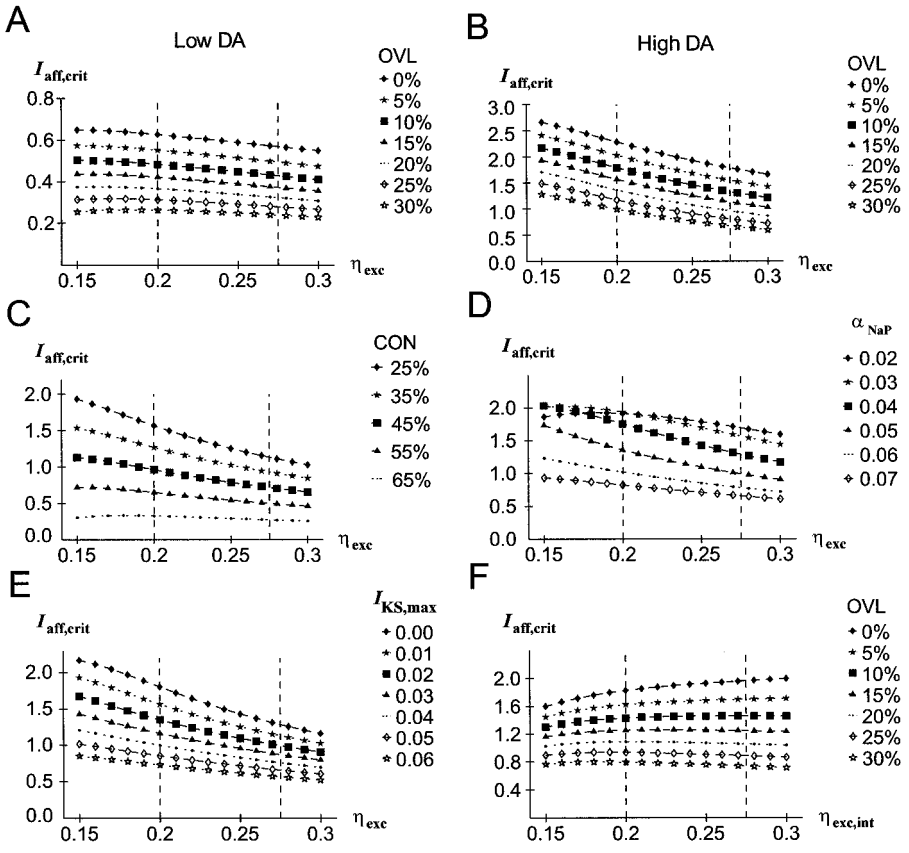

Figure 5. Effects of DA-induced variations in the general excitatory synaptic efficiency (η_{exc}) on the stability of TPs (as measured by $I_{aff,crit}$). *Dashed vertical lines* indicate the parameter range within which η_{exc} during full network simulations varied. *OVL*, Overlap; *CON*, connectivity. *A*, With all other network parameters being in a low (baseline) DA configuration, reduction of η_{exc} has only a slightly stabilizing effect at different overlaps (*CON* = 25%). *B*, With all other network parameters in a high DA configuration, reduction of η_{exc} has a >10-fold greater stabilizing effect (*CON* = 25%). *C*, In a high DA configuration, reduction of η_{exc} has a stabilizing effect at all except very high connectivities (*OVL* = 15%). *D*, The effect of a variation in η_{exc} is more pronounced at low than at high, except very low I_{NaP} activation thresholds (α_{NaP}) (*OVL* = 15%; *CON* = 25%). *E*, The effect of a variation in η_{exc} is more pronounced at low values of $I_{KS,max}$ (*OVL* = 15%; *CON* = 25%). *F*, In the high DA configuration, a reduction of η_{exc} only for PFC *internal* excitatory synapses but not for afferent synapses has a slightly stabilizing effect for high but not for low degrees of overlap (*CON* = 25%).

overlap, whereas the effect reverses at low overlaps. Thus, the change in the internal network dynamics produced by η_{exc} reduction itself does not have a consistent effect on stability (although it would if $I_{NaP,max}$ would be set very high).

Contribution of the coupling strength to stabilization of delay activity

The decrease of the coupling strength between the distal and proximal model compartment, which was meant to represent the dopaminergic modulation of a dendritic HVA Ca^{2+} current (see Materials and Methods), not surprisingly strongly diminishes the impact that intervening stimuli have on current network activity. More interestingly, this effect is much more pronounced for short-lasting distal afferent inputs than for longer-lasting inputs (Fig. 6*A*), at various degrees of overlap and connectivity (data not shown). Hence, decreasing λ_{pd} has a much bigger impact on afferent high-frequency than on low-frequency events, a result well known from passive cable theory (Spruston et al., 1993, 1994). Thus, in a high DA condition, afferent inputs to the distal dendrites not only have to be stronger [as first suggested by Yang and Seamans (1996)] but also have to be longer lasting. Only very significant and persistent stimuli may thus gain access to the working PFC network.

The implementation of the dopaminergic modulation of a dendritic HVA Ca^{2+} current by variation of the coupling strength was chosen for simplicity. This kind of implementation is reasonable in terms of the physiological effects that a DA-induced reduction of a dendritic HVA Ca^{2+} current has on the current flow from the distal to the proximal dendrites and thus on distally induced EPSPs (see Materials and Methods). Nevertheless, to further confirm the hypothesis that reduction of a dendritic HVA Ca^{2+} current reduces the impact of interfering stimuli and thus helps to stabilize currently active patterns, we also looked for the effects of modulating an explicitly modeled HVA Ca^{2+} current (I_{HVA}) inserted into the distal (apical dendrite) model compartment. This current was given a higher activation threshold than I_{NaP}, and its contribution to membrane voltage was described by:

$$V_{HVA}(V_d) = R\, I_{HVA,max}[1 + \exp(50 \times (0.1 - V_d))]^{-1}.$$

When inserted into the distal compartment, Equation 1b changes to:

$$\tau_d \dot{V}_{d,i} = -V_{d,i} + \eta_{exc} I_{af,i} + \lambda_{pd}(V_{p,i} - V_{d,i}) + V_{HVA}(V_{d,i}).$$

For the simulation runs including I_{HVA}, λ_{pd} was decreased from 0.7 to 0.2 because part of the current flow from distal to proximal results from activation of HVA Ca^{2+} channels distributed along the apical dendrites (Durstewitz and Seamans, 1997; Seamans et al., 1997).

As apparent from Figure 6*B,C*, decreasing the amplitude $I_{HVA,max}$ of the distal HVA Ca^{2+} current in fact leads to stabilization of the currently active pattern within a large range of current amplitudes for different degrees of overlap and connectivity. However, for very large values of $I_{HVA,max}$ (much larger than $I_{NaP,max}$ and $I_{KS,max}$, as given in Table 1), there is a sudden jump onto a higher level of stability where the relation between $I_{HVA,max}$ reduction and stability reverses. This occurs whenever a depolarization of the distal compartment is maintained at a very high level through almost full activation of the remote Ca^{2+} channels. This in turn could happen when the current amplitude ($I_{HVA,max}$) becomes very high or the I_{HVA} threshold becomes very low, or when there is a very loose electrotonic coupling between the proximal and the distal compartment, i.e., when λ_{pd}

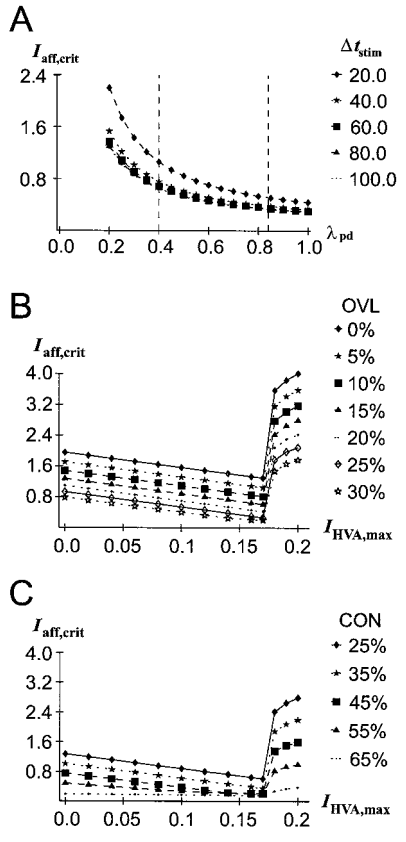

Figure 6. Effects of DA-induced variations in a dendritic "HVA Ca^{2+} channel." All other network parameters had the baseline values given in Table 1. *OVL*, Overlap; *CON*, connectivity. *A*, Decreasing the coupling strength (λ_{pd}) between the proximal and the distal "pyramidal cell" compartment diminishes the impact of intervening patterns on current network activity (as measured by $I_{aff,crit}$). This tendency is much more pronounced for short stimulus presentation times (Δt_{stim}). *OVL* = 15%; *CON* = 25%. *Dashed vertical lines* indicate the parameter range within which λ_{pd} during full network simulations varied. *B*, Reduction of the amplitude ($I_{HVA,max}$) of an explicitly modeled dendritic HVA Ca^{2+} channel has a stabilizing effect within a reasonable parameter range ($I_{HVA,max} < 0.17$) at different overlaps (*CON* = 25%). *C*, Reduction of the amplitude ($I_{HVA,max}$) of an explicitly modeled dendritic HVA Ca^{2+} channel has a stabilizing effect within a reasonable parameter range at different connectivities (*OVL* = 15%).

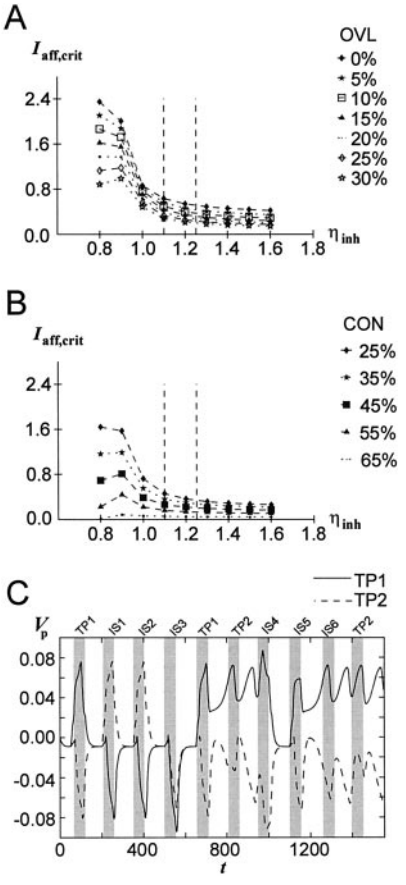

Figure 7. Effects of DA-induced variations in the inhibitory synaptic efficiency (η_{inh}) on the stability of TPs (as measured by $I_{aff,crit}$). *Dashed vertical lines* indicate the parameter range within which η_{inh} during full network simulations varied. All other network parameters had the baseline values given in Table 1. *OVL*, Overlap; *CON*, connectivity. *A*, Within the parameter range used during full network simulations, increase of η_{inh} has a mildly destabilizing effect for different overlaps (*CON* = 25%). *B*, Same as *A* for different connectivities (*OVL* = 15%). *C*, Simulation of a DMS task with the full network shows too high pyramidal cell activity peaks eventually followed by a collapse of the TP when η_{inh} (1.11) is kept constant.

gets close to 0. However, these represent rather extreme cases, so that within a physiologically reasonable parameter range reduction of $I_{HVA,max}$ increases stability, as opposed to the effect of reducing the proximally located, lower threshold I_{NaP}.

Contribution of inhibitory activity to stabilization of delay activity

An enhancement of the general inhibitory synaptic efficiency (η_{inh}), as possibly induced by DA (Rétaux et al., 1991; Yang et al., 1997), has a destabilizing effect on current delay activity, i.e., makes it easier for afferent patterns to interrupt current network activity, although this tendency is not very pronounced for the parameter range used in the full model simulations ($\eta_{inh} \geq 1.1$), and is clearly surpassed by the other DA-induced parameter changes (e.g., as evident from Fig. 2*A*). Slight destabilization occurs for various overlaps (Fig. 7*A*) and degrees of connectivity (Fig. 7*B*). The same holds for a reduction of the inhibitory unit firing threshold (θ_{inh}) (data not shown), which might represent the increased spontaneous firing frequency of GABAergic neurons under dopaminergic control (Rétaux et al., 1991). Hence, the dopaminergic modulation of GABAergic neuron activity is the only effect of DA that does not seem to fit into the present framework (but see Discussion). However, it should be mentioned that some authors have also reported a *reduction* of GABAergic currents caused by DA, not only in the basal ganglia (Bergstrom and Walters, 1984; Mercuri et al., 1985) but also in the PFC (Law-Tho et al., 1994). As apparent from Figure 7, a reduction of η_{inh} leads to higher stability of the TP and is thus consistent with the function of DA proposed here.

The DA-induced enhancement of synaptic inhibition, although having a slightly detrimental effect on TP stability, might fulfill another purpose during working memory processing. The DA-induced increase in synaptic inhibition concurrently with the other DA-induced changes may be necessary to prevent excessive excitation that could result from the enhancing effects of DA on pyramidal cell activity, i.e., may be necessary to keep the pyramidal cell activity within certain boundaries. This is illustrated in Figure 7*C*. If the baseline value of η_{inh} is slightly reduced (to 1.11) compared with the standard parameter set given in Table 1 and is not varied according to the level of DA unit output (i.e., is kept

constant), the full network driven by excitation that is too strong shows very high activity peaks during presentation of the stimuli, which like the "match enhancement" will eventually cause the TP to collapse. The DA-induced increase of η_{inh} by allowing other DA-modulated network parameters to assume more extreme values might in fact indirectly contribute to stabilization. Thus, increasing η_{inh} from 1.191 to 1.252 allows a further reduction of α_{NaP} and $I_{KS,max}$ in the high DA state via increasing the χ_{shift} (Eq. 6) for these two parameters 1.27-fold while keeping the level of delay activity below a given limit. The result is an overall increase in stability of $\Delta I_{aff,crit} \approx 0.05$, i.e., the increase in η_{inh} although it is by itself destabilizing enables a net increase in stability via further reduction of α_{NaP} and $I_{KS,max}$ (this trend was confirmed for several pairs of η_{inh}/χ_{shift} values). As illustrated next, detrimental network performance could occur even in the presence of a DA-induced enhancement of inhibition if the DA unit output is increased to supranormal levels.

Supranormal DA levels might disrupt correct network performance

Behavioral reports indicate that supranormal stimulation of D1 receptors or supranormal DA levels in the PFC, as caused by stressful events or anxiogenic drugs, might disrupt working memory performance as subnormal stimulation or DA receptor blockade does (Murphy et al., 1996a,b; Zahrt et al., 1997). Moreover, the firing frequency of delay-active PFC neurons might bear an inverse U-shaped relation to the level of DA receptor stimulation (Sawaguchi et al., 1990a,b; Williams and Goldman-Rakic, 1995). To test the idea that extreme changes in DA-modulated biophysical parameters have a destructive effect on working memory performance, the DA level in the PFC was strongly increased by setting γ_{DA} in Equation 7 to 1.9 (++DA condition). The effect of this manipulation on network performance in the DMS task can be assessed from Figure 8. Excitatory neurons in the network show premature activity peaks (Fig. 8*A*), leading in turn to premature motor responses (Fig. 8*B*) and to temporarily strongly increased inhibitory feedback. This interplay leads to uncontrolled network oscillations without any meaningful relation to the stimulus situation. The temporarily strongly decreased membrane potential of the TP units and thus temporarily weak inhibitory impact on the non-TP units also enables intervening stimuli to override the currently active representation, i.e., the current working memory content is destroyed (Fig. 8*A*, *IS1*). This fatal behavior of the network could not be prevented by letting the inhibition increase slightly stronger with the output of the DA unit than other network parameters under the ++DA condition relative to the +DA condition (i.e., setting $\gamma_{DA} > 1.9$ for η_{inh} only).

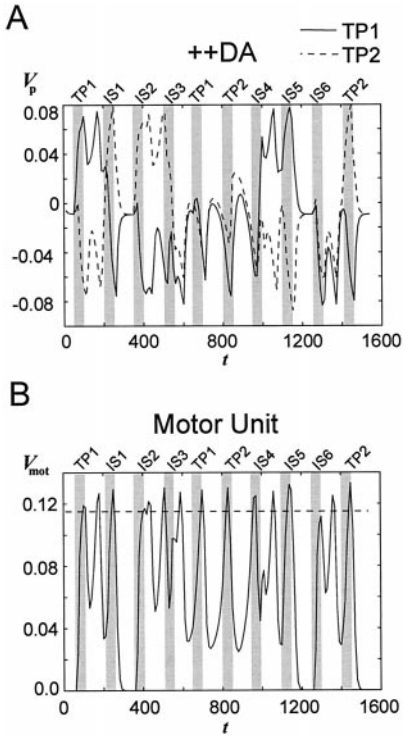

Figure 8. Activity of the PFC network under conditions of supranormal DA unit output (++*DA*) during two successive trials of a DMS task with intervening stimuli. *A*, Mean proximal membrane potential of all PFC net units belonging to the pattern "4" (=*TP1*; see Fig. 2) and pattern "0" (=*TP2*; see Fig. 2). *Gray bars* indicate the time intervals during which stimuli were presented. Three intervening stimuli were presented during each trial as described in Figure 2. The TPs are disrupted by intervening stimuli. $I_{aff} = 0.55$. *B*, Membrane potential of the motor unit, showing many premature motor responses.

DISCUSSION

To gain insights into dopaminergic functions and mechanisms during working memory processing in the PFC, a neural network model was constructed within which the dopaminergic modulation of several cellular and synaptic parameters could be implemented. Simulation results with this model network suggested that the DA-induced changes of biophysical properties of pyramidal cells and glutamatergic synapses are appropriate for stabilizing neural representations in the PFC working memory net, and thus for protecting goal-related delay activity against interfering stimuli. The dopaminergic modulation of GABAergic activity might be necessary in this context to prevent excessive excitation. Furthermore, extreme shifts in DA-modulated parameters could be as detrimental for working memory performance as no DA-induced variation at all because of uncontrolled network oscillations and premature responses. Thus, in the model net as is apparent in behavioral data (Murphy et al., 1996a; Zahrt et al., 1997), there was an optimal level of DA modulation.

Combining experimental results into a unifying explanatory neurocomputational framework

The network model presented here integrates various behavioral, neuropsychological, electrophysiological, and pharmacological *in vitro* and *in vivo* results into a unifying concept of dopaminergic functioning in the PFC and could contribute to an understanding of the biophysical mechanisms underlying this functioning. On the behavioral level, the model provides a mechanistic explanation of where the working memory and attentional deficits encountered after lesions or blockade of components of the dopaminergic input to the PFC (Brozoski et al., 1979; Simon et al., 1980; Sawaguchi and Goldman-Rakic, 1994) could come from. If no dopaminergic modulation of parameters was assumed in the model network (−DA condition in Fig. 2), active representations in the PFC net were unstable, i.e., could easily be wiped out by interfering stimulation.

Stability of active neural representations in working memory is a necessary prerequisite for (1) guiding action according to a behavioral plan or goal, (2) focusing attention on goal-relevant objects in the environment, and (3) protecting goal-related behavior against interfering stimuli or behavioral tendencies. In

terms of the neural dynamics, stable goal-related representations in PFC networks might actively suppress presently irrelevant response options or might prime representations of goal-relevant responses and sensory objects (Fuster et al., 1985; Desimone et al., 1995). Thus, according to the present neurocomputational model, various attentional and working memory disorders observed after prefrontal and dopaminergic system lesions in fact might be related to the same neural mechanism, namely to the ability of the prefrontal/dopaminergic system to stabilize neural representations. Indeed, in favor of this hypothesis, susceptibility to interference and distractibility are also prominent features of animals with prefrontal or DA system lesions, and working memory performance can generally be enhanced by reducing possible sources of interference (Montaron et al., 1982; Fuster, 1989; Roberts et al., 1994).

On a physiological level, the model might help to understand some seemingly paradoxical effects of DA. On the one hand, DA increases excitability and spike output of prefrontal pyramidal neurons via enhancing I_{NaP} and suppressing I_{KS} (Yang and Seamans, 1996). On the other hand, the DA-induced reduction of EPSP sizes and dendritic Ca^{2+} conductances acts in the opposite way, i.e., decreases excitability and spike output on synaptic stimulation. However, the model simulations suggested that all of these effects might in fact cooperate to stabilize neural representations in the PFC network. Whereas the former two effects raised the stable frequency of the TP units, thereby increasing feedback inhibition and reducing non-TP unit activation, the latter two effects diminished the impact of intervening afferent stimulation more directly. Thus, all of the DA-induced parameter changes might subserve the same function of stabilizing goal-relevant representations in working memory.

The only dopaminergic effect that does not easily fit into the present framework is that of DA on GABAergic activity. The dopaminergic modulation of GABAergic activity might have other functions during working memory processes that could compensate for the slightly detrimental effect it has on TP stability. An increase in synaptic inhibition concurrently with the DA-induced enhancement of pyramidal cell activity might be necessary simply to prevent excessive excitation that could result from the "excitatory" effects of DA. Moreover, an increase in synaptic inhibition might actually allow bigger changes in other DA-modulated parameters, thereby promoting the stabilizing effect of other DA-induced changes and increasing the net effect on stability. The dopaminergic modulation of GABAergic activity might also help to reset the working memory buffer after a goal state has been achieved, thus preventing the perseveration of TP representations. In the framework of the present model, however, this would require that the DA-induced changes in GABAergic neurons and synapses have a different time course or dynamic than the DA-induced changes in pyramidal cells and glutamatergic synapses, so that the effects on GABAergic activity persist for some time after the other DA-induced effects started to cease and/or reach a particularly high peak during the match enhancement.

Further experimental testing of model assumptions

The mean electrophysiological behavior of the delay-active model neurons matched quite well the average course of activity observed during *in vivo* recordings in the PFC (Miller et al., 1996). Moreover, a DA-induced enhancement of cue-, response-, and delay-related neural activity in working memory tasks as exhibited by the model (Fig. 2*A*) has also been demonstrated *in vivo* (Sawaguchi et al., 1988, 1990a), whereas DA receptor blockade might reduce task-related activity at high (Sawaguchi et al., 1990b) but not low (Williams and Goldman-Rakic, 1995) doses. In addition, DA increases the signal-to-noise ratio in delay activity *in vivo* (Sawaguchi et al., 1990a,b) like it increases the difference between TP and non-TP unit activity in the model. However, one critical prediction of the present model still awaits empirical confirmation. Higher doses of DA antagonists applied locally in the PFC during delay tasks with intervening stimuli should lead to a breakdown of activity of most delay-active neurons on the presentation of an intervening stimulus. In contrast, without antagonizing DA effects, activity of delay-active neurons should be *enhanced* on presentation of intervening stimuli. That is, intervening stimuli should influence current delay activity in opposite ways depending on the level of DA. To test this prediction, one would have to combine the Miller et al. (1996) task with local DA antagonist application and concurrent electrophysiological recordings. The question of whether recurrent excitation of PFC pyramidal cells is enhanced by DA and thus could provide a mechanism for stabilizing delay activity might also be addressed *in vitro* by dual cell recordings (Markram et al., 1997).

Another assumption made by the model that is open to experimental testing was that the PFC could dynamically regulate its own DA level via its efferent projections to the VTA/SN. Although this issue is not of central importance for the main hypothesis of the present model (as outlined in Materials and Methods), in our opinion, dynamic, context-dependent self-regulation of the prefrontal DA level provides a very interesting theoretical possibility, and the temporal relationship between the onset of stimulus-related and delay activity in the PFC and in the SN/VTA should be investigated *in vivo.*

Extensions of the present model

The present work showed that the DA-induced biophysical changes are, in principle, appropriate for stabilizing neural representations in the PFC network during working memory tasks. To show this, a model on a relatively high level of biological abstraction was chosen. This model had the advantage that the biophysical mechanisms leading to the proposed function of DA in working memory could be analyzed and understood relatively easily. However, as a next step, it should be confirmed that the same functional effects of DA also hold in a network of biologically very detailed compartmental model neurons (Durstewitz and Seamans, 1997; Durstewitz, 1998). In a more detailed network model it might also be possible to find a functional interpretation for the DA-induced changes in GABAergic unit activity. For example, increased GABAergic interneuron activity and IPSP sizes (Rétaux et al., 1991; Yang et al., 1997) might induce a mode of synchronous oscillations in which GABAergic interneurons probably play an important role (Lytton and Sejnowski, 1991; Cobb et al., 1995; Bush and Sejnowski, 1996). This mode of synchronous oscillations, besides providing a representational medium (Singer, 1993; König et al., 1996), might indeed have an additional stabilizing effect on current delay activity. This is a question that cannot be examined with the present model neurons with their mean frequency output.

In conclusion, it is predicted that the role of DA is to stabilize critical, goal-related delay activity and to protect it against interfering stimulation and response tendencies, regardless of the kind of working memory task used. In addition, we would like to point out that the function of DA proposed here might not be restricted

fto working memory processes, because stable, maintained neural activity probably plays an important role in many sensory motor processes and operant learning situations in which DA is involved (Salamone, 1992, 1994; Beninger, 1993).

APPENDIX

We will show here that an additional source of current, as provided by the DA-induced enhancement of the persistent Na^+ current, present in *all* model neurons will push the stable frequency of the delay-active TP units to higher values and will increase the difference in membrane potential between the TP and the non-TP units. To show this, we make the following assumptions. (1) The network is in an attractor state with suprathreshold delay activity, i.e.: $dV_p/dt = dV_d/dt = dV_{inh}/dt = 0$, and $V_p > \theta_{exc}$ for all TP neurons. (2) For all non-TP units, $f_{exc} = 0$. This will usually be the case if some TP is active, and neither $I_{NaP,max}$ nor the connectivity or the overlap between the TP and the intervening pattern become too high. (3) $f_{inh} > 0$. This, again, should usually be the case if a TP is active, because otherwise excitation could spread throughout the entire network. (4) For simplicity, we will furthermore assume that I_{KS} (and thus V_{KS}) is a constant. Assuming (1), the distal membrane potential is given by:

$$V_d = \frac{V_p}{1/\lambda_{pd} + 1} + \frac{\eta_{exc} I_{aff}}{1+\lambda_{pd}}. \quad (8)$$

Inserting Equations 4 and 8 into Equation 1a, we get for the proximal membrane potential in the stable state:

$$a_1 V_{p,i} = \eta_{exc} \sum_{j \neq i}^{N} w_{ij} f_{exc}(V_{p,j}) - \eta_{inh}\left(\frac{1}{N_S}\eta_{exc}\sum_{j}^{N} f_{exc}(V_{p,j}) - \theta_{inh}\right) + V_{NaP} + V_{KS} + a_2, \quad (9)$$

with $a_1 = (2\lambda_{pd} + 1)/(\lambda_{pd} + 1) > 0$ for $\lambda_{pd} \geq 0$ and $a_2 = (\lambda_{pd}\eta_{exc} I_{aff})/(\lambda_{pd} + 1)$. If synaptic connectivity is strictly defined by the Willshaw matrix (Eq. 5), then all the delay-active excitatory neurons receive exactly the same input and settle at the same stable frequency $f_{exc} > 0$. Thus, Equation 9 simplifies to:

$$a_1 V_p = \eta_{exc} w (N_S - 1) f_{exc}(V_p) - \eta_{inh}\eta_{exc} f_{exc}(V_p) + \eta_{inh}\theta_{inh} + V_{NaP} + V_{KS} + a_2 = (\eta_{exc} - \eta_{inh}\eta_{exc}) f_{exc}(V_p) + \eta_{inh}\theta_{inh} + V_{NaP} + V_{KS} + a_2. \quad (10)$$

Inserting Equation 3 into Equation 10, we can rewrite this equation as:

$$-b_1 V_p + b_2 + b_3 I_{NaP} = \ln(V_p), \quad (11)$$

with $b_1 = -a_1/(\eta_{exc} - \eta_{inh}\eta_{exc}) > 0$, $b_2 = \ln(\theta_{exc}) - (\eta_{inh}\theta_{inh} + V_{KS} + a_2)/(\eta_{exc} - \eta_{inh}\eta_{exc})$, and $b_3 = -R/(\eta_{exc} - \eta_{inh}\eta_{exc}) > 0$ (provided that $\eta_{inh} > 1$ as in Table 1; if $\eta_{inh} < 1$, both b_1 and b_3 become negative, in which case an analysis can be performed analog to the one presented here, leading to the same results). The solutions of this equation are the intersections of the straight line on the left-hand side and the logarithmic function on the right-hand side, as plotted in Figure 9. For the parameter settings used in the present simulations ($\eta_{inh} > 1$), only one intersection and thus only one solution exists. This solution is a stable state (fix point attractor) of the network (Amit and Brunel, 1995). Indicating the intersection with V_X, this can be shown by verifying that $dV_p/dt > 0$ for $V_p \in]\theta_{exc}; V_X[$ and $dV_p/dt < 0$ for $V_p > V_X$, because of the fact that the logarithmic function lies below the straight line for $V_p < V_X$, and lies above it for $V_p > V_X$.

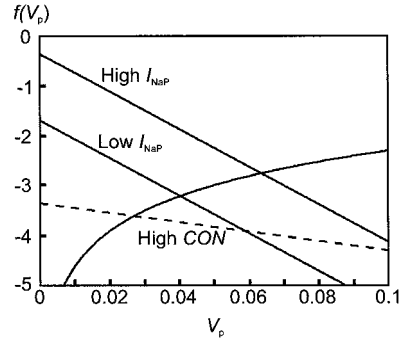

Figure 9. The *crossings* of the logarithmic function with the *straight lines* give the stable membrane potential of the TP units for conditions of low $I_{NaP,cons}$ (=0.04), high $I_{NaP,cons}$ (=0.09), and high connectivity ($I_{NaP,cons}$ = 0.04) where the non-TP units become active above threshold.

Now one can see directly from Equation 11 that increasing I_{NaP}, as accomplished by DA, will move the straight line in a positive direction on the *y*-axis as shown in Figure 9. Thus, the intersection V_X moves to the right, i.e., the stable membrane potential and hence the stable frequency increase. For the neurons not involved in encoding the target stimulus, the situation looks quite different. For these (non-TP) neurons, the proximal membrane potential in the stable state is given by:

$$a_1 V_{p,non\text{-}TP} = (CON \times \eta_{exc} - \eta_{inh}\eta_{exc}) f_{exc}(V_{p,TP}) + \eta_{inh}\theta_{inh} + V_{NaP} + V_{KS} + a_2, \quad (12)$$

where CON denotes here the relative (*to* $N_S - 1$) number of inputs that the respective non-TP unit receives from TP units, because of an overlap between the patterns or the "pure" connectivity as defined in Materials and Methods (note that $V_{p,non\text{-}TP}$ does not occur on the right-hand side). Note that the assumptions made at the beginning imply that CON < 1.0. Comparing Equation 12 with 10, one sees that by increasing I_{NaP} for all neurons, the difference in membrane potential between the TP and the non-TP units will increase by an amount [1 − CON] $\eta_{exc}\Delta f_{exc}$, where Δf_{exc} is the increase in the stable frequency of the TP units attributable to the enhanced I_{NaP}. Thus, providing an additional source of excitatory current to all model neurons enlarges the difference between TP and non-TP unit activation.

Note that this analysis strictly holds only under the assumption that $f_{exc} = 0$ for the non-TP units. If too many network units become active close in time, as it happens with too high connectivites or too high values of constant I_{NaP} injection, the stable membrane potential decreases (as illustrated by the *dotted line* in Fig. 9) and may be temporarily pushed below the excitatory threshold by the fast rising inhibitory feedback. (Even in cases in which the stable frequency still lies above the excitatory threshold, in the dynamic model the membrane potential may be pushed below it, depending on the time constants of the excitatory and inhibitory units.)

REFERENCES

Abercrombie ED, Keefe KA, DiFrischia DS, Zigmond MJ (1989) Differential effect of stress on in vivo dopamine release in striatum, nucleus accumbens, and medial frontal cortex. J Neurochem 52:1655–1658.

Alzheimer C, Schwindt PC, Crill WE (1993) Modal gating of Na^+

channels as a mechanism of persistent Na^+ current in pyramidal neurons from rat and cat sensorimotor cortex. J Neurosci 13:660–673.
Amit DJ (1995) The Hebbian paradigm reintegrated: local reverberations as internal representations. Behav Brain Sci 18:617–657.
Amit DJ, Brunel N (1995) Learning internal representations in an attractor neural network with analogue neurons. Network 6:359–388.
Amit DJ, Brunel N, Tsodyks MV (1994) Correlations of cortical Hebbian reverberations: theory versus experiment. J Neurosci 14:6435–6445.
Amit DJ, Fusi S, Yakovlev V (1997) Paradigmatic working memory (attractor) cell in IT cortex. Neural Comput 9:1071–1092.
Arnsten AF, Cai JX, Murphy BL, Goldman-Rakic PS (1994) Dopamine D1 receptor mechanisms in the cognitive performance of young and aged monkeys. Psychopharmacology (Berl) 116:143–151.
Beninger RJ (1993) Role of D_1 and D_2 receptors in learning. In: D_1:D_2 dopamine receptor interactions (Waddington JL, ed), pp 115–157. London: Academic.
Berger B, Trottier S, Verney C, Gaspar P, Alvarez C (1988) Regional and laminar distribution of the dopamine and serotonin innervation in the macaque cerebral cortex: a radioautographic study. J Comp Neurol 273:99–119.
Berger B, Febvret A, Greengard P, Goldman-Rakic PS (1990) DARPP-32, a phosphoprotein enriched in dopaminoceptive neurons bearing dopamine D1 receptors: distribution in the cerebral cortex of the newborn and adult rhesus monkey. J Comp Neurol 299:327–348.
Berger B, Gaspar P, Verney C (1991) Dopaminergic innervation of the cerebral cortex: unexpected differences between rodents and primates. Trends Neurosci 14:21–27.
Bergstrom DA, Walters JR (1984) Dopamine attenuates the effects of GABA on single unit activity in the globus pallidus. Brain Res 310:23–33.
Bernander Ö, Koch C, Douglas RJ (1994) Amplification and linearization of distal synaptic input to cortical pyramidal cells. J Neurophysiol 12:2743–2753.
Bernardi G, Cherubini E, Marciani MG, Mercuri N, Stanzione P (1982) Responses of intracellularly recorded cortical neurons to the iontophoretic application of dopamine. Brain Res 245:267–274.
Blaha CD, Yang CR, Floresco SB, Barr AM, Phillips AG (1997) Stimulation of the ventral subiculum of the hippocampus evokes glutamate receptor-mediated changes in dopamine efflux in the rat nucleus accumbens. Eur J Neurosci 9:902–911.
Brown AM, Schwindt PC, Crill WE (1994) Different voltage dependence of transient and persistent Na^+ currents is compatible with modal-gating hypothesis for sodium channels. J Neurophysiol 71:2562–2565.
Brozoski TJ, Brown RM, Rosvold HE, Goldman PS (1979) Cognitive deficit caused by regional depletion of dopamine in prefrontal cortex of rhesus monkey. Science 205:929–932.
Bush P, Sejnowski TJ (1996) Inhibition synchronizes sparsely connected cortical neurons within and between columns in realistic network models. J Comput Neurosci 3:91–110.
Carter CJ (1982) Topographical distribution of possible glutamatergic pathways from the frontal cortex to the striatum and substantia nigra in rats. Neuropharmacology 21:379–383.
Cauller LJ (1995) Layer I of primary sensory neocortex: where top-down converges upon bottom-up. Behav Brain Res 71:163–170.
Cauller LJ, Clancy B, Connors BW (1998) Backward cortical projections to primary somatosensory cortex in rats extend long horizontal axons in layer I. J Comp Neurol 390:297–310.
Cepeda C, Radisavljevic Z, Peacock W, Levine MS, Buchwald NA (1992) Differential modulation by dopamine of responses evoked by excitatory amino acids in human cortex. Synapse 11:330–341.
Cepeda C, Chandler SH, Shumate LW, Levine MS (1995) Persistent Na^+ conductance in medium-sized neostriatal neurons: characterization using infrared videomicroscopy and whole-cell patch-clamp recordings. J Neurophysiol 74:1343–1348.
Cobb SR, Buhl EH, Halasy K, Paulsen O, Somogyi P (1995) Synchronization of neuronal activity in hippocampus by individual GABAergic interneurons. Nature 378:75–78.
Constantinidis C, Steinmetz MA (1996) Neuronal activity in posterior parietal area 7a during the delay periods of a spatial memory task. J Neurophysiol 76:1352–1355.
Cummins TR, Xia Y, Haddad GG (1994) Functional properties of rat and human neocortical voltage-sensitive sodium currents. J Neurophysiol 71:1052–1064.
Desimone R, Miller EK, Chelazzi L, Lueschow A (1995) Multiple memory systems in the visual cortex. In: The cognitive neurosciences (Gazzaniga MS, ed), pp 475–486. Cambridge, MA: MIT.
Di Pellegrino G, Wise SP (1993) Visuospatial versus visuomotor activity in the premotor and prefrontal cortex of a primate. J Neurosci 13:1227–1243.
Douglas RJ, Martin KAC (1990) Neocortex. In: The synaptic organization of the brain (Shepherd GM, ed), pp 389–438. Oxford: Oxford UP.
Durstewitz D (1998) Die dopaminerge Modulation von Arbeitsgedächtnisprozessen: Neurocomputationale Studien und Untersuchungen am Endhirn der Taube (*Columba livia*) (The dopaminergic modulation of working memory processes: neurocomputational studies and investigations of the pigeon telencephalon). Ph.D. thesis, Ruhr-Universität Bochum.
Durstewitz D, Seamans JK (1997) The possible function of dendritic HVA calcium channels in prefrontal cortical pyramidal cells: a combined *in vitro* electrophysiological and compartmental modeling study. Soc Neurosci Abstr 23:1188.
Durstewitz D, Kröner S, Hemmings HC, Güntürkün O (1998) The dopaminergic innervation of the pigeon telencephalon: distribution of DARPP-32 and co-occurrence with glutamate decarboxylase and tyrosine hydroxylase. Neuroscience 83:763–779.
Ferron A, Thierry AM, Le Douarin C, Glowinski J (1984) Inhibitory influence of the mesocortical dopaminergic system on spontaneous activity or excitatory response induced from the thalamic mediodorsal nucleus in the rat medial prefrontal cortex. Brain Res 302:257–265.
Fleidervish IA, Friedman A, Gutnick MJ (1996) Slow inactivation of Na^+ current and slow cumulative spike adaptation in mouse and guinea-pig neocortical neurones in slices. J Physiol (Lond) 493.1:83–97.
Formenti A, Martina M, Plebani A, Mancia M (1998) Multiple modulatory effects of dopamine on calcium channel kinetics in adult rat sensory neurons. J Physiol (Lond) 509.2:395–409.
Funahashi S, Kubota K (1994) Working memory and prefrontal cortex. Neurosci Res 21:1–11.
Fuster JM (1973) Unit activity in prefrontal cortex during delayed-response performance: neuronal correlates of transient memory. J Neurophysiol 36:61–78.
Fuster JM (1989) The prefrontal cortex: anatomy, physiology, and neuropsychology of the frontal lobe. New York: Raven.
Fuster JM, Bauer RH, Jervey JP (1985) Functional interactions between inferotemporal and prefrontal cortex in a cognitive task. Brain Res 330:299–307.
Godbout R, Mantz J, Pirot S, Glowinski J, Thierry A-M (1991) Inhibitory influence of the mesocortical dopaminergic neurons on their target cells: electrophysiological and pharmacological characterization. J Pharmacol Exp Ther 258:728–738.
Goldman-Rakic PS (1990) Cellular and circuit basis of working memory in prefrontal cortex of nonhuman primates. In: Progress in brain research (Uylings HBM, Van Eden CG, De Bruin JPC, Corner MA, Feenstra MGP, eds), pp 325–336. Oxford: Elsevier.
Goldman-Rakic PS (1995) Toward a circuit model of working memory and the guidance of voluntary motor action. In: Models of information processing in the basal ganglia (Houk JC, Davis JL, Beiser DG, eds), pp 131–148. Cambridge, MA: MIT.
Goldman-Rakic PS, Leranth C, Williams SM, Mons N, Geffard M (1989) Dopamine synaptic complex with pyramidal neurons in primate cerebral cortex. Proc Natl Acad Sci USA 86:9015–9019.
Goldman-Rakic PS, Bates JF, Chafee MV (1992a) The prefrontal cortex and internally generated motor acts. Curr Opin Neurobiol 2:830–835.
Goldman-Rakic PS, Lidow MS, Smiley JF, Williams MS (1992b) The anatomy of dopamine in monkey and human prefrontal cortex. J Neural Transm 36:163–177.
Goldstein LE, Rasmusson AM, Bunney BS, Roth RH (1996) Role of the amygdala in the coordination of behavioral, neuroendocrine, and prefrontal cortical monoamine responses to psychological stress in the rat. J Neurosci 16:4787–4798.
Gonon FG (1988) Nonlinear relationship between impulse flow and dopamine released by rat midbrain dopaminergic neurons as studied by in vivo electrochemistry. Neuroscience 24:19–28.
Gorelova N, Yang CR (1997) Dopamine D1 receptor stimulation modulates a slowly inactivating Na^+ current in layer V–VI prefrontal cortical (PFC) neurons. Soc Neurosci Abstr 23:1771.
Gulledge AT, Jaffe DB (1998) Dopamine decreases the excitability of layer V pyramidal cells in the rat prefrontal cortex. J Neurosci 18:9139–9151.

Heimer L, Zahm DS, Alheid GF (1995) Basal ganglia. In: The rat nervous system (Paxinos G, ed), pp 579–628. San Diego: Academic.
Hikosaka O, Wurtz RH (1983) Visual and oculomotor functions of monkey substantia nigra pars reticulata. III. Memory-contingent visual and saccade responses. J Neurophysiol 49:1268–1284.
Huguenard JR, Prince DA (1991) Slow inactivation of a TEA-sensitive K current in acutely isolated rat thalamic relay neurons. J Neurophysiol 66:1316–1328.
Jones EG (1984) Laminar distribution of cortical efferent cells. In: Cerebral cortex (Peters A, Jones EG, eds), pp 521–552. New York: Plenum.
Joyce JN, Goldsmith S, Murray A (1993) Neuroanatomical localization of D_1 versus D_2 receptors: similar organization in the basal ganglia of the rat, cat and human and disparate organization in the cortex and limbic system. In: D_1:D_2 dopamine receptor interactions (Waddington JL, ed), pp 23–49. London: Academic.
Karreman M, Moghaddam B (1996) The prefrontal cortex regulates the basal release of dopamine in the limbic striatum: an effect mediated by ventral tegmental area. J Neurochem 66:589–598.
Kesner RP, Hunt ME, Williams JM, Long JM (1996) Prefrontal cortex and working memory for spatial response, spatial location, and visual object information in the rat. Cereb Cortex 6:311–318.
König P, Engel AK, Singer W (1996) Integrator or coincidence detector? The role of the cortical neuron revisited. Trends Neurosci 19:130–137.
Kornhuber J, Kim JS, Kornhuber ME, Kornhuber HH (1984) The cortico-nigral projection: reduced glutamate content in the substantia nigra following frontal cortex ablation in the rat. Brain Res 322:124–126.
Kritzer MF, Goldman-Rakic PS (1995) Intrinsic circuit organization of the major layers and sublayers of the dorsolateral prefrontal cortex in the rhesus monkey. J Comp Neurol 359:131–143.
Law-Tho D, Hirsch JC, Crepel F (1994) Dopamine modulation of synaptic transmission in rat prefrontal cortex: an in vitro electrophysiological study. Neurosci Res 21:151–160.
Levitt JB, Lewis DA, Yoshioka T, Lund J (1993) Topography of pyramidal neuron intrinsic connections in macaque monkey prefrontal cortex (area 9 and 46). J Comp Neurol 338:360–376.
Lewis DA, Hayes TL, Lund JS, Oeth KM (1992) Dopamine and the neural circuitry of primate prefrontal cortex: implications for schizophrenia research. Neuropsychopharmacology 6:127–134.
Ljungberg T, Apicella P, Schultz W (1992) Responses of monkey dopamine neurons during learning of behavioral reactions. J Neurophysiol 67:145–163.
Lübke J, Markram H, Frotscher M, Sakmann B (1996) Frequency and dendritic distribution of autapses established by layer V pyramidal neurons in the developing rat neocortex: comparison with synaptic innervation of adjacent neurons of the same class. J Neurosci 16:3209–3218.
Lytton WW, Sejnowski TJ (1991) Simulations of cortical pyramidal neurons synchronized by inhibitory interneurons. J Neurophysiol 66:1059–1079.
Mantz J, Milla C, Glowinski J, Thierry AM (1988) Differential effects of ascending neurons containing dopamine and noradrenaline in the control of spontaneous activity and of evoked responses in the rat prefrontal cortex. Neuroscience 27:517–526.
Markram H, Lübke J, Frotscher M, Roth A, Sakmann B (1997) Physiology and anatomy of synaptic connections between thick tufted pyramidal neurones in the developing rat neocortex. J Physiol (Lond) 500.2:409–440.
Mercuri N, Bernardi G, Calabresi P, Cotugno A, Levi G, Stanzione P (1985) Dopamine decreases cell excitability in rat striatal neurons by pre- and postsynaptic mechanisms. Brain Res 358:110–121.
Miller EK, Desimone R (1994) Parallel neuronal mechanisms for short-term memory. Science 263:520–522.
Miller EK, Li L, Desimone R (1991) A neural mechanism for working and recognition memory in inferior temporal cortex. Science 254:1377–1379.
Miller EK, Li L, Desimone R (1993) Activity of neurons in anterior inferior temporal cortex during a short-term memory task. J Neurosci 13:1460–1478.
Miller EK, Erickson CA, Desimone R (1996) Neural mechanisms of visual working memory in prefrontal cortex of the macaque. J Neurosci 16:5154–5167.
Mitchell BD, Cauller LJ (1997) Cortico-cortical and thalamocortical projections to layer I of the prefrontal/premotor neocortex in rats. Soc Neurosci Abstr 23:1273.
Mittmann T, Linton SM, Schwindt P, Crill W (1997) Evidence for persistent Na^+ current in apical dendrites of rat neocortical neurons from imaging of Na^+-sensitive dye. J Neurophysiol 78:1188–1192.
Montaron M-F, Bouyer J-J, Rougeul A, Buser P (1982) Ventral mesencephalic tegmentum (VMT) controls electrocortical beta rhythms and associated attentive behaviour in the cat. Behav Brain Res 6:129–145.
Moore H, Lavin A, Grace AA (1998) Interactions between dopamine and NMDA delivered locally by microdialysis during *in vivo* intracellular recordings of rat prefrontal cortical neurons. Soc Neurosci Abstr 24:2061.
Müller U, von Cramon DY, Pollmann S (1998) D1- versus D2-receptor modulation of visuospatial working memory in humans. J Neurosci 18:2720–2728.
Muly III EC, Szigeti K, Goldman-Rakic PS (1998) D_1 receptor in interneurons of macaque prefrontal cortex: distribution and subcellular localization. J Neurosci 18:10553–10565.
Murase S, Grenhoff J, Chouvet G, Gonon FG, Svensson TH (1993) Prefrontal cortex regulates burst firing and transmitter release in rat mesolimbic dopamine neurons studied in vivo. Neurosci Lett 157:53–56.
Murphy BL, Arnsten AFT, Goldman-Rakic PS, Roth RH (1996a) Increased dopamine turnover in the prefrontal cortex impairs spatial working memory performance in rats and monkeys. Proc Natl Acad Sci USA 93:1325–1329.
Murphy BL, Arnsten AFT, Jentsch JD, Roth RH (1996b) Dopamine and spatial working memory in rats and monkeys: pharmacological reversal of stress-induced impairment. J Neurosci 16:7768–7775.
Nishino H, Hattori S, Muramoto K, Ono T (1991) Basal ganglia neural activity during operant feeding behavior in the monkey: relation to sensory integration and motor execution. Brain Res Bull 27:463–468.
Passingham R (1975) Delayed matching after selective prefrontal lesions in monkeys (*Macaca mulatta*). Brain Res 92:89–102.
Penit-Soria J, Audinat E, Crepel F (1987) Excitation of rat prefrontal cortical neurons by dopamine: an in vitro electrophysiological study. Brain Res 425:263–274.
Petrides M (1995) Impairments on nonspatial self-ordered and externally ordered working memory tasks after lesions of the mid-dorsal part of the lateral frontal cortex in the monkey. J Neurosci 15:359–375.
Pirot S, Godbout R, Mantz J, Tassin J-P, Glowinski J, Thierry A-M (1992) Inhibitory effects of ventral tegmental area stimulation on the activity of prefrontal cortical neurons: evidence for the involvement of both dopaminergic and GABAergic components. Neuroscience 49:857–865.
Pirot S, Glowinski J, Thierry A-M (1996) Mediodorsal thalamic evoked responses in the rat prefrontal cortex: influence of the mesocortical DA system. NeuroReport 7:1437–1441.
Pralong E, Jones RSG (1993) Interactions of dopamine with glutamate- and GABA-mediated synaptic transmission in the rat entorhinal cortex in vitro. Eur J Neurosci 5:760–767.
Press WH, Teukolsky SA, Vetterling WT, Flannery BP (1992) Numerical recipes in C. Cambridge: Cambridge UP.
Quintana J, Yajeya J, Fuster JM (1988) Prefrontal representation of stimulus attributes during delay tasks. I. Unit activity in cross-temporal integration of sensory and sensory-motor information. Brain Res 474:211–221.
Rétaux S, Besson MJ, Penit-Soria J (1991) Opposing effects of dopamine D2 receptor stimulation on the spontaneous and the electrically evoked release of [^{3}H]GABA on rat prefrontal cortex slices. Neuroscience 42:61–71.
Richardson NR, Gratton A (1998) Changes in medial prefrontal cortical dopamine levels associated with response-contingent food reward: an electrochemical study in rat. J Neurosci 18:9130–9138.
Roberts AC, De Salvia MA, Wilkinson LS, Collins P, Muir JL, Everitt BJ, Robbins TW (1994) 6-Hydroxydopamine lesions of the prefrontal cortex in monkeys enhance performance on an analog of the Wisconsin Card Sorting Test: possible interactions with subcortical dopamine. J Neurosci 14:2531–2544.
Salamone JD (1992) Complex motor and sensorimotor functions of striatal and accumbens dopamine: involvement in instrumental behavior processes. Psychopharmacology 107:160–174.
Salamone JD (1994) The involvement of nucleus accumbens dopamine in appetitive and aversive motivation. Behav Brain Res 61:117–133.

Sawaguchi T, Goldman-Rakic PS (1991) D1 dopamine receptors in prefrontal cortex: involvement in working memory. Science 251:947–950.
Sawaguchi T, Goldman-Rakic PS (1994) The role of D1-dopamine receptor in working memory: local injections of dopamine antagonists into the prefrontal cortex of rhesus monkeys performing an oculomotor delayed-response task. J Neurophysiol 71:515–528.
Sawaguchi T, Matsumura M, Kubota K (1988) Dopamine enhances the neuronal activity of spatial short-term memory task in the primate prefrontal cortex. Neurosci Res 5:465–473.
Sawaguchi T, Matsumura M, Kubota K (1990a) Catecholaminergic effects on neuronal activity related to a delayed response task in monkey prefrontal cortex. J Neurophysiol 63:1385–1400.
Sawaguchi T, Matsumura M, Kubota K (1990b) Effects of dopamine antagonists on neuronal activity related to a delayed response task in monkey prefrontal cortex. J Neurophysiol 63:1401–1412.
Schiller J, Schiller Y, Stuart G, Sakmann B (1997) Calcium action potentials restricted to distal apical dendrites of rat neocortical pyramidal neurons. J Physiol (Lond) 505:605–616.
Schultz W (1992) Activity of dopamine neurons in the behaving primate. Semin Neurosci 4:129–138.
Schultz W, Romo R (1990) Dopamine neurons of the monkey midbrain: contingencies of responses to stimuli eliciting immediate behavioral reactions. J Neurophysiol 63:607–624.
Schultz W, Apicella P, Ljungberg T (1993) Responses of monkey dopamine neurons to reward and conditioned stimuli during successive steps of learning a delayed response task. J Neurosci 13:900–913.
Schwindt PC, Crill WE (1995) Amplification of synaptic current by persistent sodium conductance in apical dendrite of neocortical neurons. J Neurophysiol 74:2220–2224.
Schwindt P, Crill W (1996) Equivalence of amplified current flowing from dendrite to soma measured by alteration of repetitive firing and by voltage clamp in layer 5 pyramidal neurons. J Neurophysiol 76:3731–3739.
Seamans JK, Gorelova NA, Yang CR (1997) Contributions of voltage-gated Ca^{2+} channels in the proximal versus distal dendrites to synaptic integration in prefrontal cortical neurons. J Neurosci 17:5936–5948.
Seamans JK, Floresco SB, Phillips AG (1998) D1 receptor modulation of hippocampal–prefrontal cortical circuits integrating spatial memory with executive functions in the rat. J Neurosci 18:1613–1621.
Selemon LD, Goldman-Rakic PS (1985) Longitudinal topography and interdigitation of corticostriatal projections in the rhesus monkey. J Neurosci 5:776–794.
Sesack SR, Bunney BS (1989) Pharmacological characterization of the receptor mediating electrophysiological responses to dopamine in the rat medial prefrontal cortex: a microiontophoretic study. J Pharmacol Exp Ther 248:1323–1333.
Shi W-X, Zheng P, Liang X-F, Bunney BS (1997) Characterization of dopamine-induced depolarization of prefrontal cortical neurons. Synapse 26:415–422.
Simon H, Scatton B, Le Moal M (1980) Dopaminergic A10 neurones are involved in cognitive functions. Nature 286:150–151.
Singer W (1993) Synchronization of cortical activity and its putative role in information processing and learning. Annu Rev Neurosci 55:349–374.
Smiley JF, Goldman-Rakic PS (1993) Heterogeneous targets of dopamine synapses in monkey prefrontal cortex demonstrated by serial section electron microscopy: a laminar analysis using the silver-enhanced diaminobenzidine sulfide (SEDS) immunolabeling technique. Cereb Cortex 3:223–238.
Spain WJ, Schwindt PC, Crill WE (1991) Two transient potassium currents in layer V pyramidal neurones from cat sensorimotor cortex. J Physiol (Lond) 434:591–607.
Spruston N, Jaffe DB, Williams SH, Johnston D (1993) Voltage- and space-clamp errors associated with the measurement of electrotonically remote synaptic events. J Neurophysiol 70:781–802.
Spruston N, Jaffe DB, Johnston D (1994) Dendritic attenuation of synaptic potentials and currents: the role of passive membrane properties. Trends Neurosci 17:161–166.
Stuart G, Sakmann B (1995) Amplification of EPSPs by axosomatic sodium channels in neocortical pyramidal neurons. Neuron 15:1065–1076.
Surmeier DJ, Bargas J, Hemmings HCJ, Nairn AC, Greengard P (1995) Modulation of calcium currents by a D_1 dopaminergic protein kinase/phosphatase cascade in rat neostriatal neurons. Neuron 14:385–397.
Tong Z-Y, Overton PG, Clark D (1996a) Stimulation of the prefrontal cortex in the rat induces patterns of activity in midbrain dopaminergic neurons which resemble natural burst events. Synapse 22:195–208.
Tong Z-Y, Overton PG, Clark D (1996b) Antagonism of NMDA but not AMPA/kainate receptors blocks bursting in dopaminergic neurons induced by electrical stimulation of the prefrontal cortex. J Neural Transm 103:889–905.
Watanabe M, Kodama T, Hikosaka K (1997) Increase of extracellular dopamine in primate prefrontal cortex during a working memory task. J Neurophysiol 78:2795–2798.
Westenbroek RE, Merrick DK, Catterall WA (1989) Differential subcellular localization of the R_I and R_{II} Na^+ channel subtypes in central neurons. Neuron 3:695–704.
Westenbroek RE, Hell JW, Warner C, Dubel SJ, Snutch TP, Catterall WA (1992) Biochemical properties and subcellular distribution of an N-type calcium channel a1 subunit. Neuron 9:1099–1115.
Williams GV, Goldman-Rakic PS (1995) Modulation of memory fields by dopamine D1 receptors in prefrontal cortex. Nature 376:572–575.
Yang CR, Seamans JK (1996) Dopamine D1 receptor actions in layers V–VI rat prefrontal cortex neurons *in vitro*: modulation of dendritic–somatic signal integration. J Neurosci 16:1922–1935.
Yang CR, Seamans JK, Gorelova N (1996) Focal dendritic D1 receptor stimulation differentially modulates layers I–II and V–VI glutamate inputs to deep layer prefrontal cortical (PFC) pyramidal neurons *in vitro.* Soc Neurosci Abstr 22:1770.
Yang CR, Seamans JK, Gorelova N (1997) Mechanisms of dopamine (DA) modulation of GABAergic inputs to rat layer V–VI pyramidal prefrontal cortical (PFC) neurons *in vitro.* Soc Neurosci Abstr 23:1771.
Yuste R, Gutnick MJ, Saar D, Delaney KR, Tank DW (1994) Ca^{2+} accumulations in dendrites of neocortical pyramidal neurons: an apical band and evidence for two functional compartments. Neuron 13:23–43.
Zahrt J, Taylor JR, Mathew RG, Arnsten AFT (1997) Supranormal stimulation of D_1 dopamine receptors in the rodent prefrontal cortex impairs spatial working memory performance. J Neurosci 17:8528–8535.